

Electronic Supplementary Information

Pyrrole-based anion-responsive π -electronic molecules as fluorescence sensors responsive to multiple stimuli

Shinya Sugiura and Hiromitsu Maeda*

Department of Applied Chemistry, College of Life Sciences, Ritsumeikan University, Kusatsu 525–8577, Japan, Fax: +81 77 561 2659; Tel: +81 77 561 5969; E-mail: maedahir@ph.ritsumei.ac.jp

Table of Contents

1. Spectroscopic data	S2
Fig. S1,2 ^1H and ^{13}C NMR spectra.	S2
Fig. S3,4 UV/vis absorption and fluorescence spectra.	S4
2. X-ray crystallographic data	S5
Fig. S5,6 Ortep and packing drawings of single-crystal X-ray structure.	S5
3. Theoretical study	S7
Fig. S7,8 Optimized structures.	S7
Fig. S9,10 Molecular orbitals.	S8
Fig. S11–14 TD-DFT calculations.	S9
Cartesian coordination of optimized structures	S11
4. Anion-binding and protonation behaviors	S18
Fig. S15–20 ^1H NMR spectral changes upon the addition of Cl^- or TFA.	S18
Fig. S21–28 UV/vis absorption spectral changes and corresponding titration plots upon the addition of anions or TFA.	S22
Fig. S29–36 Fluorescence spectral changes upon the addition of Cl^- or TFA.	S26
Fig. S37 ^1H NMR spectral changes upon the addition of Cl^- and TFA.	S29
Fig. S38–45 UV/vis absorption and fluorescence spectral changes upon the addition of Cl^- and TFA.	S29

1. Synthetic procedures and spectroscopic data

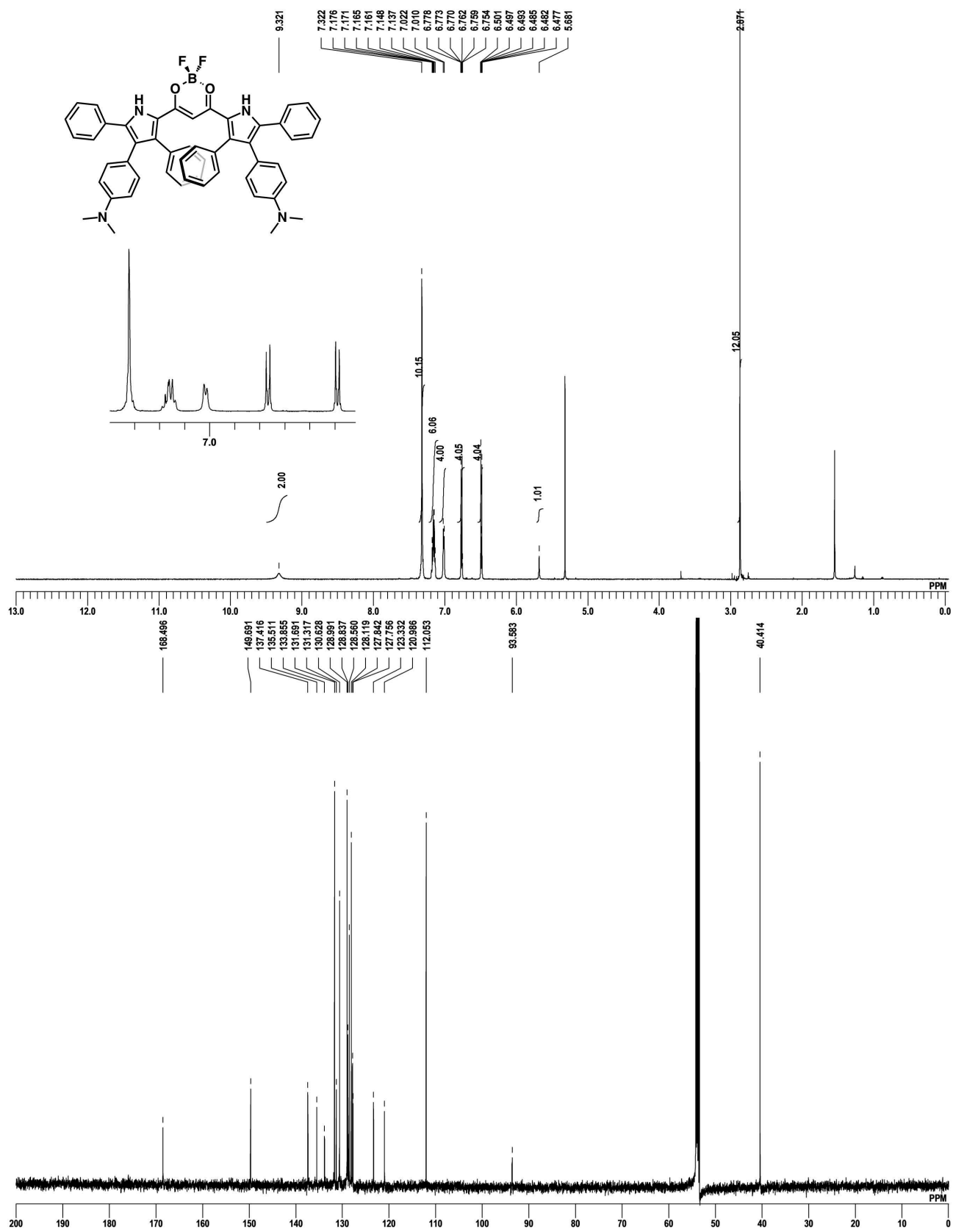


Fig. S1 ^1H NMR (top) and ^{13}C NMR (bottom) spectra of **3a** in CD_2Cl_2 at 20°C . The detailed data are described in the experimental section.

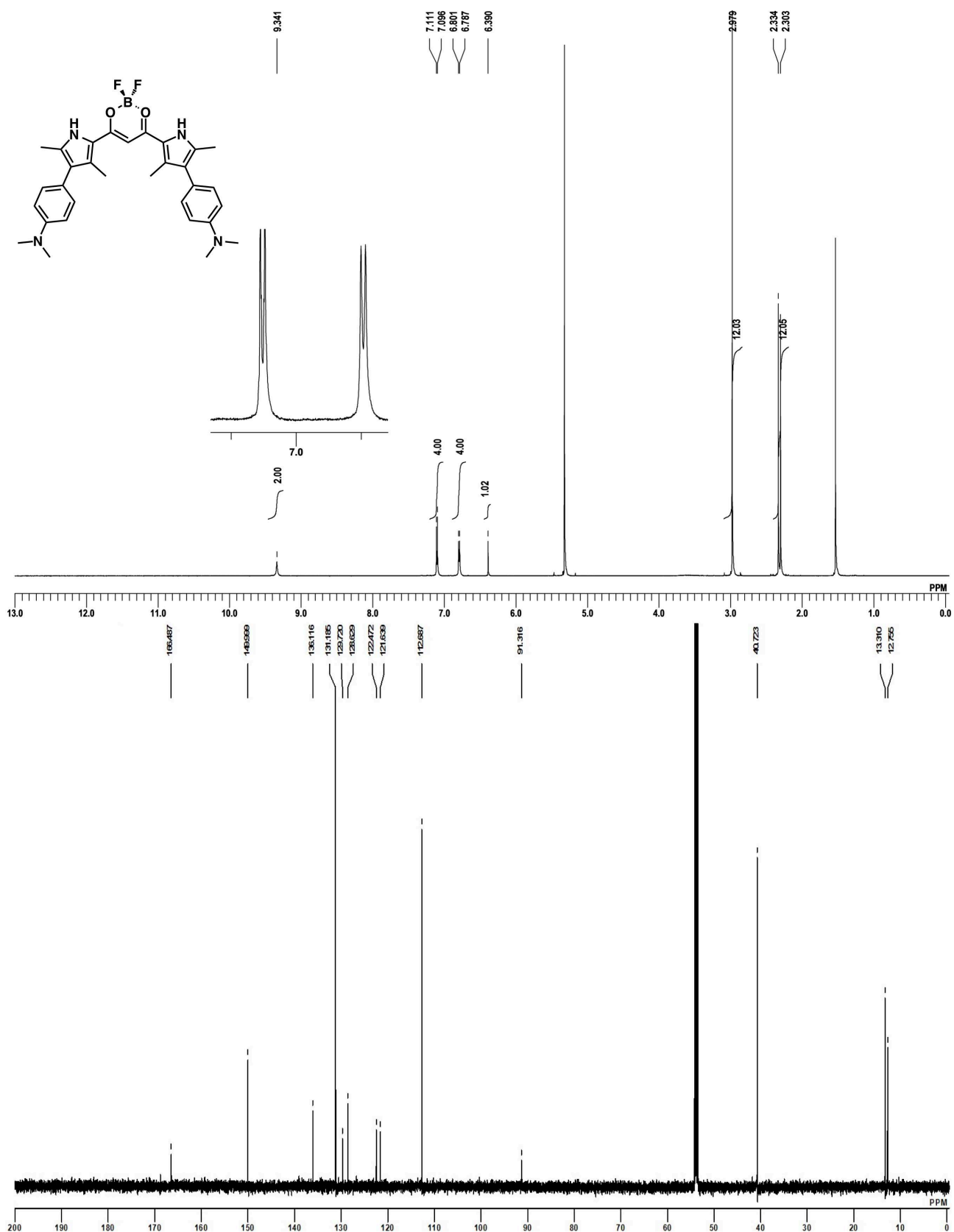


Fig. S2 ¹H NMR (top) and ¹³C NMR (bottom) spectra of **3b** in CD₂Cl₂ at 20 °C. The detailed data are described in the experimental section.

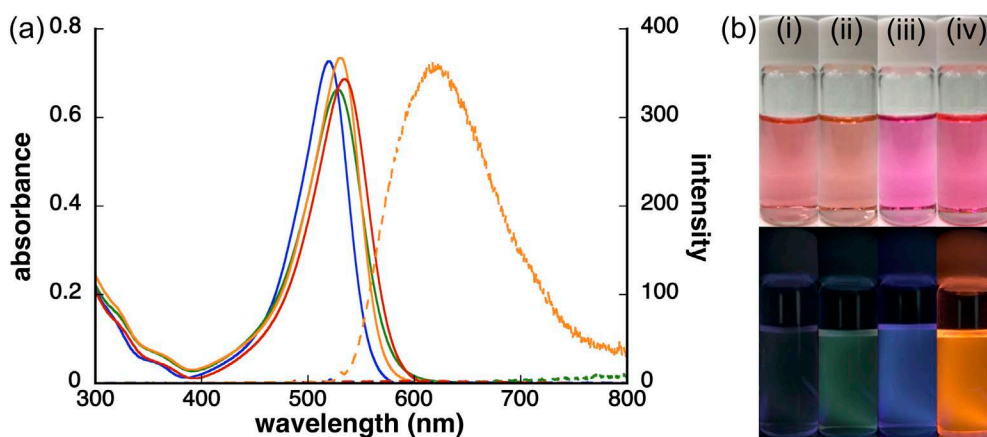


Fig. S3 (a) UV/vis absorption (solid line) and fluorescence spectra (broken line) of **3a** (1.0×10^{-5} M), excited at the absorption maxima, in CH₂Cl₂ (dielectric constant ϵ_r : 8.93; green, λ_{\max} = 528 nm), THF (ϵ_r : 7.58; blue, λ_{\max} = 520 nm), CHCl₃ (ϵ_r : 4.81; red, λ_{\max} = 535 nm), and toluene (ϵ_r : 2.38; orange, λ_{\max} = 531 nm, λ_{em} = 630 nm) and (b) the corresponding photographs under visible light (top) and 365-nm UV light (bottom) in (i) CH₂Cl₂, (ii) THF, (iii) CHCl₃, and (iv) toluene under the conditions for spectral measurements. Fluorescence quantum yields (Φ_{FL}) are estimated as 0.001 (CH₂Cl₂), 0.000 (THF), 0.017 (CHCl₃), and 0.29 (toluene).

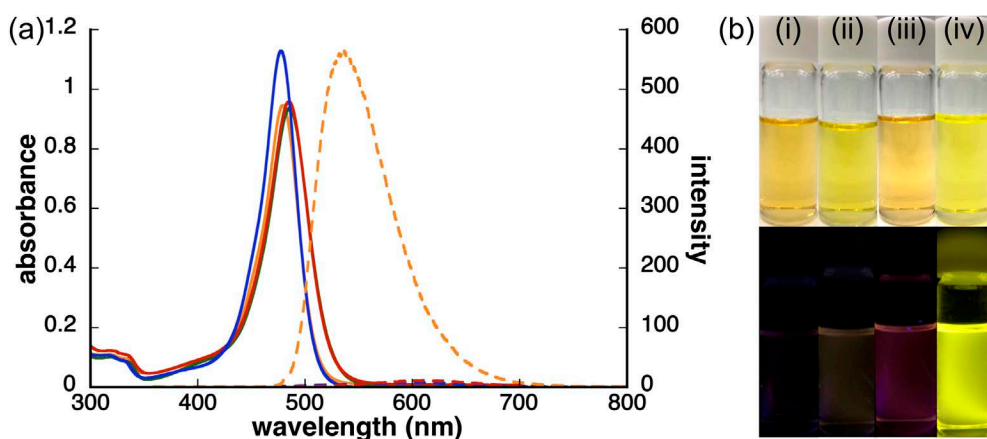


Fig. S4 (a) UV/vis absorption (solid line) and fluorescence spectra (broken line) of **3b** (1.0×10^{-5} M), excited at the absorption maxima, in CH₂Cl₂ (ϵ_r : 8.93; green, λ_{\max} = 485 nm), THF (ϵ_r : 7.58; blue, λ_{\max} = 478 nm), CHCl₃ (ϵ_r : 4.81; red, λ_{\max} = 485 nm), and toluene (ϵ_r : 2.38; orange, λ_{\max} = 480 nm, λ_{em} = 535 nm) and (b) the corresponding photographs under visible light (top) and 365-nm UV light (bottom) in (i) CH₂Cl₂, (ii) THF, (iii) CHCl₃, and (iv) toluene under the conditions for spectral measurements. Φ_{FL} are estimated as 0.013 (CH₂Cl₂), 0.034 (THF), 0.047 (CHCl₃), and 0.47 (toluene).

2. X-ray crystallographic data

Table S1 Crystallographic details.

3a	
formula	C ₅₁ H ₄₃ BF ₂ N ₄ O ₂ ·2C ₄ H ₈ O ₂
fw	968.91
crystal size, mm	1.000 × 0.050 × 0.050
crystal system	monoclinic
space group	C2/c (no. 15)
<i>a</i> , Å	27.487(2)
<i>b</i> , Å	11.9733(10)
<i>c</i> , Å	19.9835(17)
α , °	90
β , °	132.480(9)
γ , °	90
<i>V</i> , Å ³	4850.4(9)
ρ_{calcd} , gcm ⁻³	1.639
<i>Z</i>	4
<i>T</i> , K	100(2)
μ , mm ⁻¹	0.038
no. of reflns	71568
no. of unique reflns	5577
variables	330
λ , Å	0.4115
<i>R</i> ₁ (<i>I</i> > 2 σ (<i>I</i>))	0.0385
<i>wR</i> ₂ (<i>I</i> > 2 σ (<i>I</i>))	0.1017
<i>GOF</i>	1.053

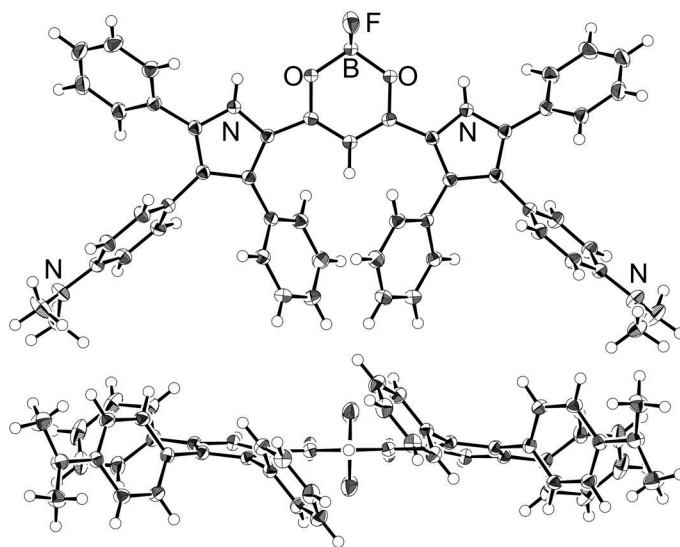


Fig. S5 Ortep drawing of single-crystal X-ray structure (top and side views) of 3a. Thermal ellipsoids are scaled to the 50% probability level. Solvent molecules are omitted for clarity.

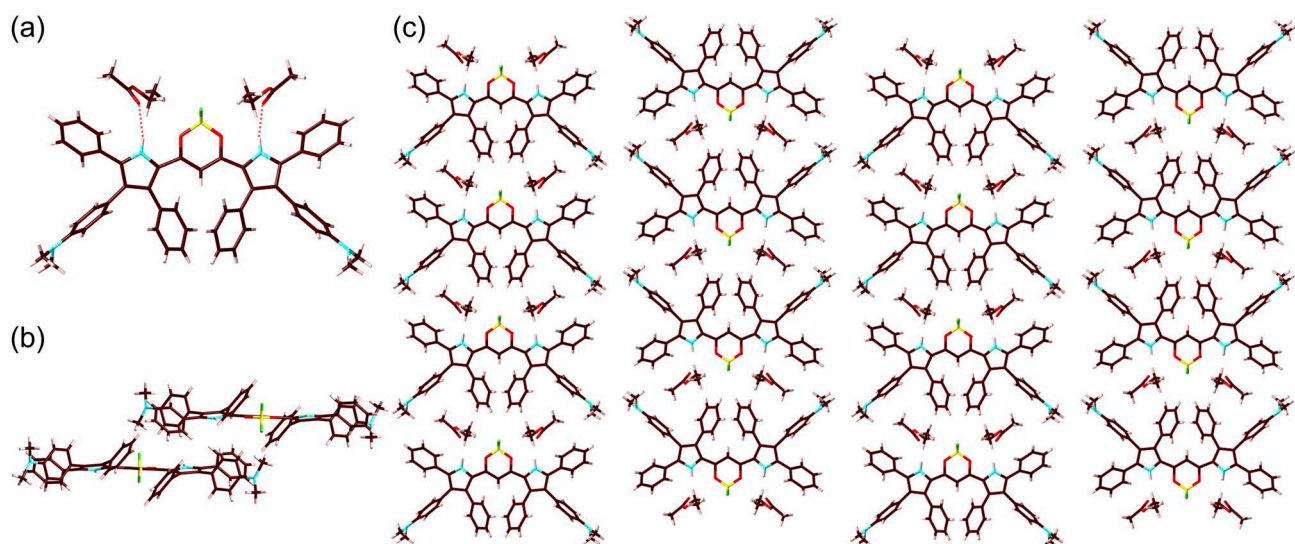


Fig. S6 Packing diagrams of **3a**: (a) a hydrogen-bonding structure with an N(-H)···O distance of 2.922 Å, (b) a stacking with a π-π distance of 4.396 Å, which was estimated by using the average distance between mean planes of five- and six-membered rings (pyrrole and core 1,3-diketone boron complex, respectively), suggesting the absence of π-π interaction in the solid state, and (c) packing diagram. Atom color code: brown, pink, yellow, blue, red, and green refer to carbon, hydrogen, boron, nitrogen, oxygen, and fluorine, respectively.

3. Theoretical study

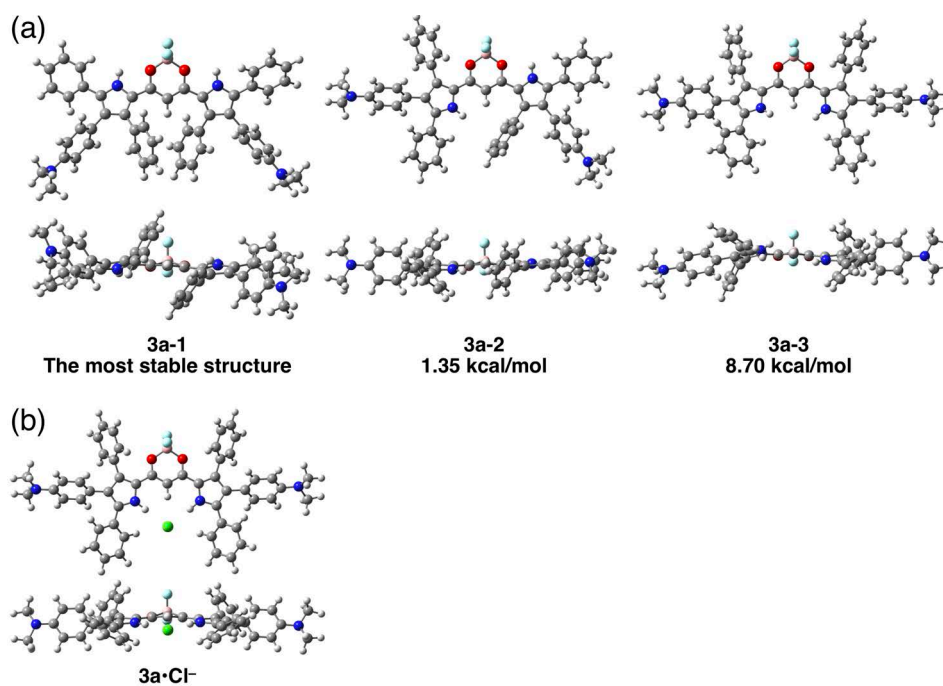


Fig. S7 Optimized structures (top and side views) of (a) **3a** (**3a-1**: pyrrole-non-inverted conformation; **3a-2**: one-pyrrole-inverted conformation; **3a-3**: two-pyrrole-inverted conformation) and (b) **3a·Cl⁻** at B3LYP/6-31+G(d,p). The difference in energy changes by the pyrrole inversion from **3a-1** to **3a-2** and that from **3a-2** to **3a-3** is probably due to the release of sterical hindrance of 3-phenyl moieties in **3a-1** by the first pyrrole inversion.

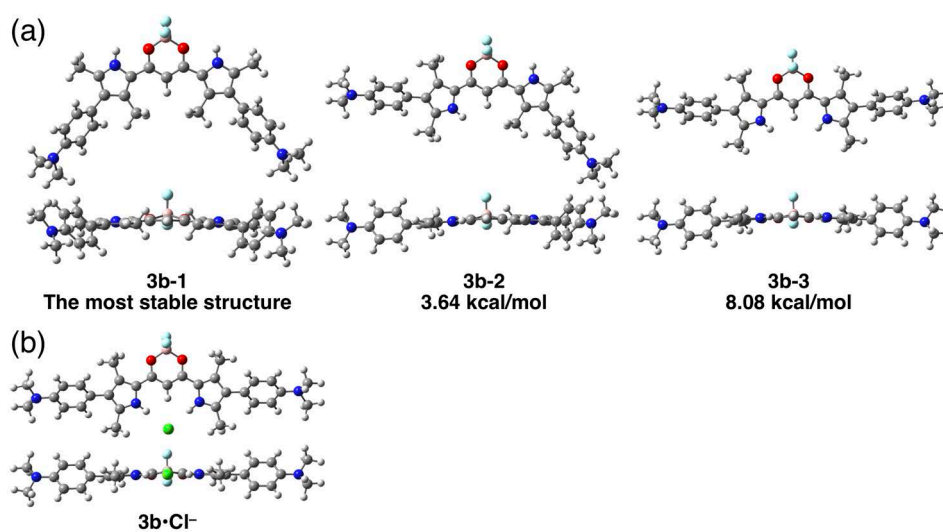


Fig. S8 Optimized structures (top and side views) of (a) **3b** (**3b-1**: pyrrole-non-inverted conformation; **3b-2**: one-pyrrole-inverted conformation; **3b-3**: two-pyrrole-inverted conformation) and (b) **3b·Cl⁻** at B3LYP/6-31+G(d,p).

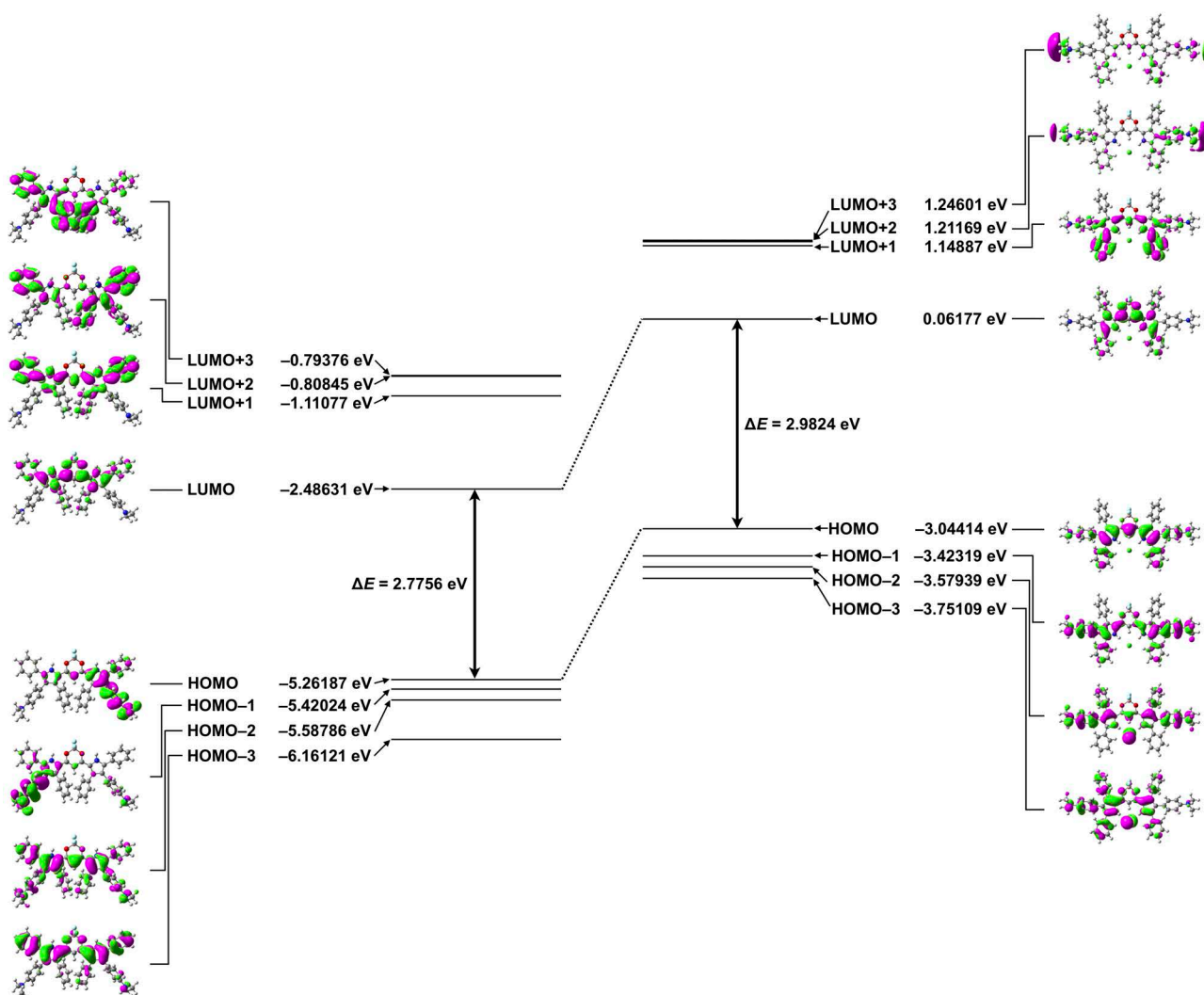


Fig. S9 Molecular orbitals (HOMO/LUMO) of **3a** (left) and **3a·Cl⁻** (right) estimated at B3LYP/6-31+G(d,p).

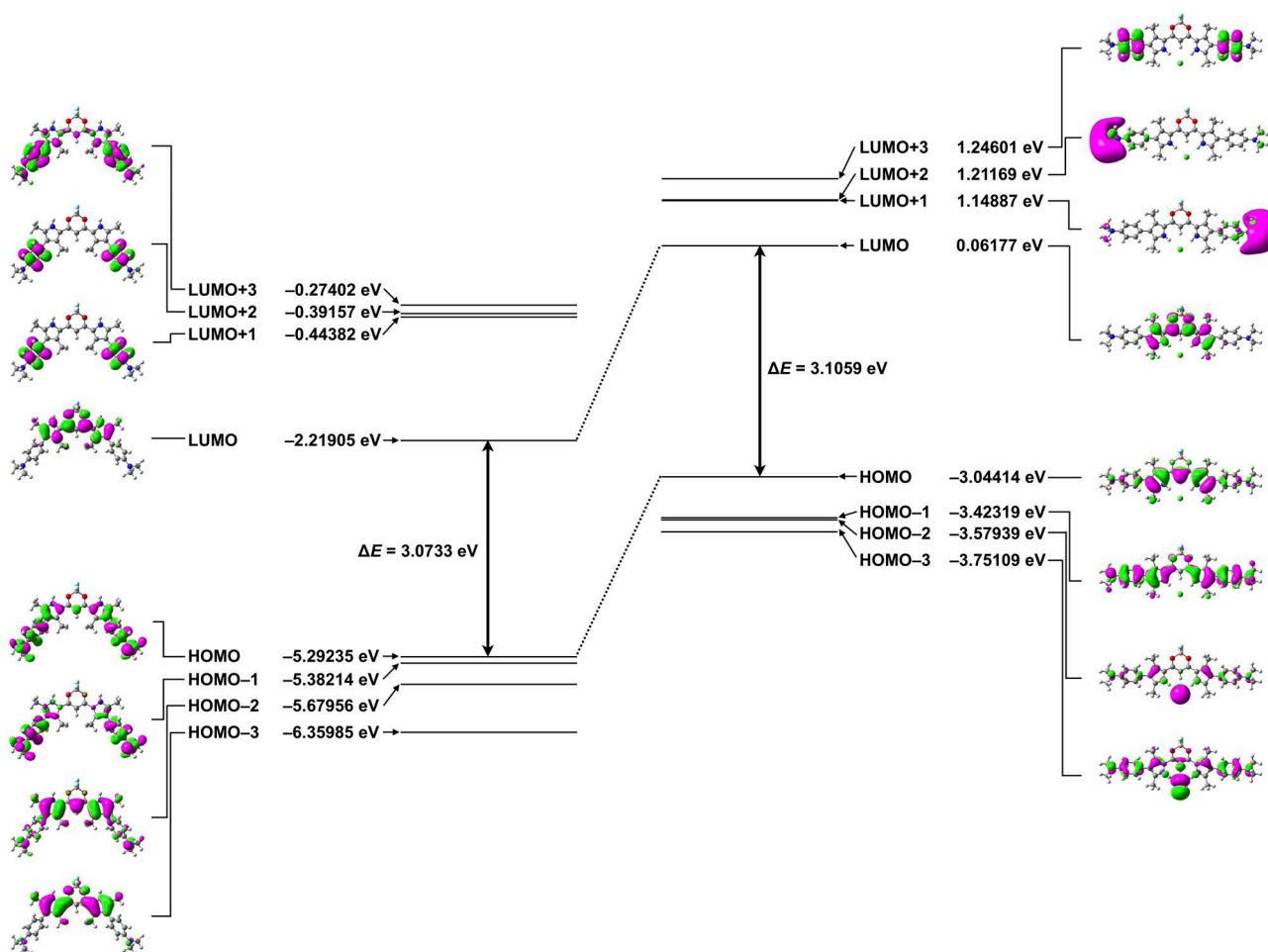


Fig. S10 Molecular orbitals (HOMO/LUMO) of **3b** (left) and **3b**·Cl⁻ (right) estimated at B3LYP/6-31+G(d,p).

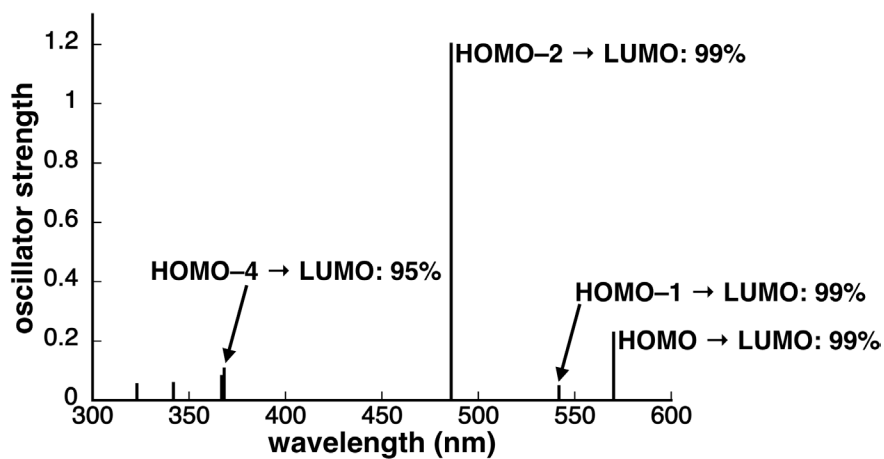


Fig. S11 TD-DFT-based UV/vis absorption stick spectrum of **3a** with the transitions correlated with molecular orbitals (MOs) estimated at PCM-B3LYP/6-31+G(d,p)(CH₂Cl₂)/B3LYP/6-31+G(d,p).

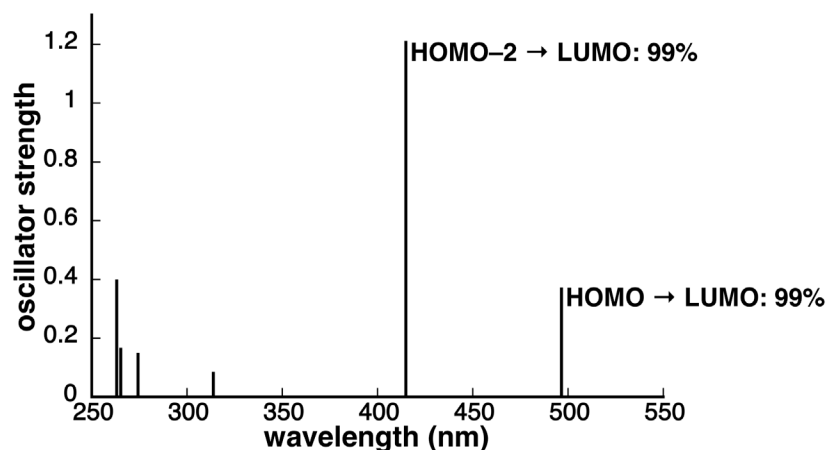


Fig. S12 TD-DFT-based UV/vis absorption stick spectrum of **3b** with the transitions correlated with MOs estimated at PCM-B3LYP/6-31+G(d,p)(CH₂Cl₂)/B3LYP/6-31+G(d,p).

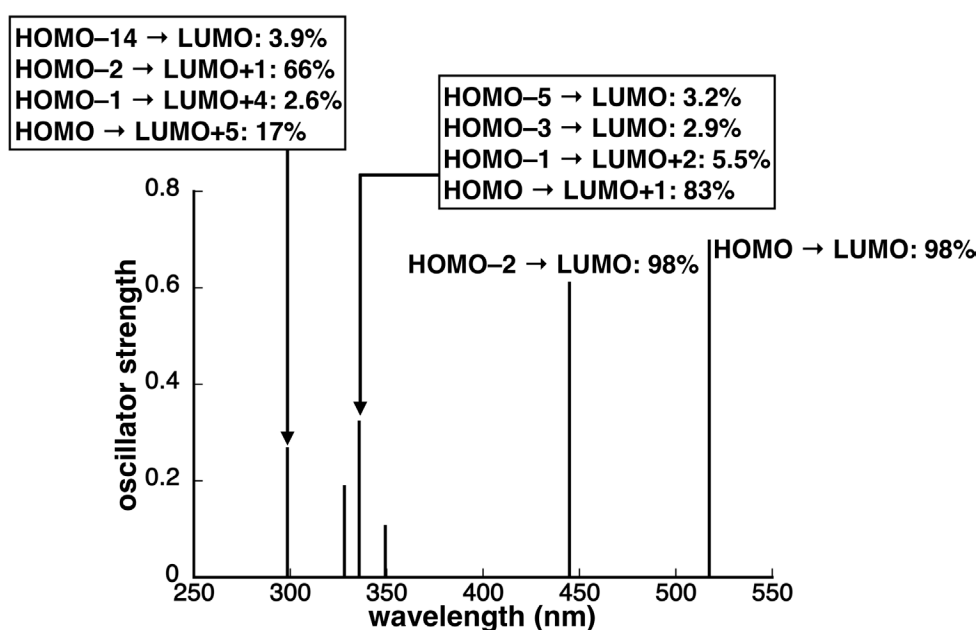


Fig. S13 TD-DFT-based UV/vis absorption stick spectrum of **3a·Cl⁻** with the transitions correlated with MOs estimated at PCM-B3LYP/6-31+G(d,p)(CH₂Cl₂)/B3LYP/6-31+G(d,p).

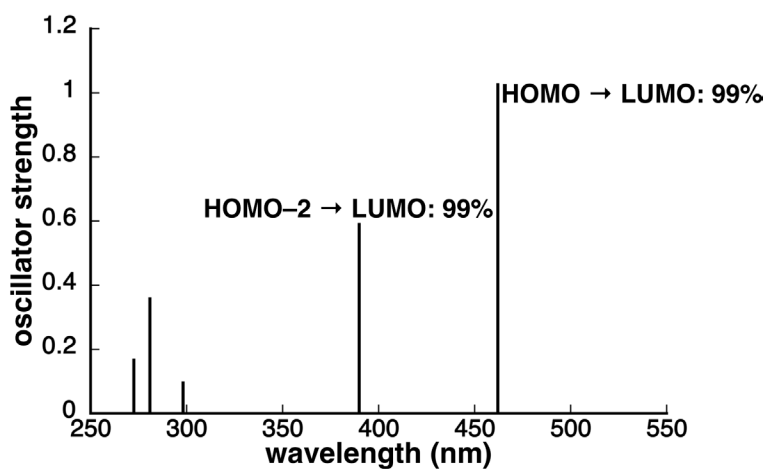


Fig. S14 TD-DFT-based UV/vis absorption stick spectrum of **3b·Cl⁻** with the transitions correlated with MOs estimated at PCM-B3LYP/6-31+G(d,p)(CH₂Cl₂)/B3LYP/6-31+G(d,p).

Cartesian Coordination of 3a-1

-2563.6979197 hartree
H,-3.4258054453,3.2861489952,-0.7427857003
H,3.4591632231,3.3493234291,0.5782933887
O,-1.2183506876,3.4421163606,-0.0774802168
O,1.2136243196,3.4506972828,0.0886409669
F,0.0200290745,5.3876565642,-0.4641810463
F,-0.1173497916,4.547052652,1.6802484225
C,-1.2111358032,2.1283905945,0.0444828813
C,4.4597122053,0.357806708,-0.0339700101
C,-2.5252641987,1.5384373499,-0.0108136786
C,-4.4457529792,0.3120068444,-0.0763379305
C,-0.0066813221,1.4214555401,0.1348081187
C,1.1966273364,2.1334188928,0.0875144803
C,2.5169556094,1.5484883663,0.0562549322
B,-0.0284827343,4.2611106892,0.3232686445
N,-3.5676197546,2.334021615,-0.4346052346
N,3.5754118632,2.3606406099,0.4026117221
C,-3.0582185686,0.2601621033,0.249555439
C,3.0485839468,0.2775278397,-0.2346408047
H,-0.0048115667,0.3439723046,0.1873283798
C,2.326620334,-0.9121729925,-0.742440875
C,1.5723986917,-0.8375567795,-1.9269933673
C,2.4415312592,-2.1556214158,-0.0987242294
C,0.9554975551,-1.973426018,-2.4541254498
H,1.4853731094,0.1138631182,-2.4435446784
C,1.8254681212,-3.2911070657,-0.6268297735
H,3.0213064541,-2.2299855274,0.8156409397
C,1.0838656339,-3.2058739285,-1.8078217857
H,0.3826758384,-1.8957695683,-3.3740532761
H,1.92706902,-4.2433850354,-0.1142052552
H,0.609518264,-4.0915568087,-2.2210087738
C,-2.3741622301,-0.8621640348,0.9336484917
C,-1.8160402236,-0.6629770531,2.2100980857
C,-2.316941635,-2.1481939319,0.373855001
C,-1.2213784026,-1.7174426464,2.9036305591
H,-1.8625299587,0.3233377261,2.6622256378
C,-1.7243112942,-3.2039931336,1.0693124525
H,-2.7303579703,-2.3199325787,-0.6136780683
C,-1.1765807191,-2.9941910024,2.3366222121
H,-0.8005446229,-1.5421619194,3.889696383
H,-1.6882559108,-4.1904778851,0.6163169904
H,-0.7170304893,-3.8167275154,-2.8772228335
C,4.7533279863,1.6781236279,0.3591225182
C,-4.7297832913,1.6254758933,-0.5011174844
C,6.0213332527,2.3509441422,0.6788519224
C,6.0654303833,3.34805769,1.6723136708
C,7.2049493339,2.0446962024,-0.0180347536
C,7.2539226681,4.022135172,1.9555470246
H,5.17146708,3.5810790022,2.2443852512
C,8.3915587034,2.7175101659,0.2713975944
H,7.1883626251,1.2866081926,-0.7928725934
C,8.4227027238,3.7093409514,1.2567280154
H,7.2666480818,4.7857020836,2.7278451631
H,9.2937230503,2.4713171183,-0.2812038245
H,9.3484555941,4.2324234454,1.4776095119
C,-5.9809330761,2.2713486573,-0.9200719608
C,-6.9846249018,1.5546884627,-1.5984130543
C,-6.1930616847,3.6406229045,-0.6630590093
C,-8.1565406275,2.189984275,-2.0079289026

H,-6.8411146113,0.5016861844,-1.8095845987
C,-7.3640345144,4.2733205523,-1.0799977359
H,-5.4524341182,4.2097043624,-0.1080097756
C,-8.3519151253,3.5508909017,-1.7547111585
H,-8.917179043,1.6196032844,-2.5332353001
H,-7.5077983006,5.328676754,-0.867498451
H,-9.265153653,4.0424230658,-2.0768649895
C,5.439204274,-0.7426721623,-0.1945067921
C,6.2601286655,-1.1503558432,0.8683990247
C,5.5937027407,-1.4205601737,-1.4136008064
C,7.1899055753,-2.177714988,0.7296080903
H,6.1744161053,-0.650485498,1.829337002
C,6.5179372863,-2.4503549244,-1.5710278352
H,4.9835199138,-1.1328818575,-2.2648808963
C,7.3374148191,-2.8690275562,-0.4961719133
H,7.7968559667,-2.440619889,1.587007565
H,6.5943211345,-2.927482839,-2.5400986387
C,-5.4437610595,-0.7711973928,0.1204548107
C,-6.2937942339,-0.7799677793,1.2361422229
C,-5.5864328737,-1.8241647081,-0.7946645556
C,-7.240484635,-1.7821428984,1.433395145
H,-6.2100283752,0.0136660246,1.9735238867
C,-6.5287919917,-2.8348801721,-0.6166563525
H,-4.951835636,-1.8538591897,-1.6767036825
C,-7.3940442288,-2.8365200776,0.5026433543
H,-7.8591465876,-1.736444452,2.3209571653
H,-6.5849382616,-3.6218029752,-1.3586015427
N,-8.3630983151,-3.8215986068,0.672040302
N,8.2360615605,-3.9237531328,-0.6333439876
C,-9.0488507926,-3.9261181061,1.9513588153
H,-9.791510334,-4.723485592,1.8921800713
H,-8.3650981521,-4.1495319345,2.7865717973
H,-9.582299875,-2.9990894582,2.1857219399
C,-8.3068163397,-5.0179915814,-0.153981686
H,-9.1527333732,-5.6611414571,0.0940734789
H,-8.3892099557,-4.7651831197,-1.2163512789
H,-7.3783902351,-5.5945898111,-0.0094294425
C,9.2356168624,-4.1399660472,0.4015676635
H,9.8305354025,-5.0176191131,0.1434125327
H,9.9175371499,-3.2824815174,0.5242419266
H,8.761816153,-4.3390255447,1.3685766761
C,8.530205989,-4.4336161213,-1.9637846123
H,9.2249494279,-5.2707547416,-1.877855307
H,7.6228346103,-4.8094719645,-2.44805776
H,8.981872532,-3.6746156357,-2.6236002683

Cartesian Coordination of 3a-2

-2563.6957656 hartree
H,-1.5050218544,-0.812148427,-0.6764525969
H,3.5050802586,3.4786887356,-0.6823095526
O,-1.2258287624,3.1713577468,-1.0031896793
O,1.2109134514,3.3600591121,-0.9165634184
F,-0.1202807091,5.1182879278,-1.6931221154
F,-0.1620102816,4.5754330101,0.5515406952
C,-1.1288784835,1.9048250355,-0.6968965421
C,4.6104508991,0.5089128419,-0.1322243596
C,-2.3546799575,1.1441371796,-0.6815194495
C,-4.494266518,0.3479838117,-0.6946108021
C,0.1231639588,1.3212225449,-0.4353596929
C,1.2807590463,2.0831231528,-0.6068656569

C,2.6286771252,1.5859459294,-0.4688792368
B,-0.0859420493,4.1151294641,-0.7587174762
N,-2.3367846945,-0.2407731926,-0.6939952961
N,3.6587595399,2.4997061653,-0.4815611232
C,-3.7070533717,1.53856093,-0.6854380803
C,3.203671832,0.3198276072,-0.2549251739
H,0.2101818022,0.2939885677,-0.118983271
C,2.4949328955,-0.9799523937,-0.152231493
C,1.8623623292,-1.5469219336,-1.2722292462
C,2.4605562911,-1.6809565437,1.0639931251
C,1.2021656597,-2.7743068206,-1.1738966871
H,1.8950887916,-1.0218138919,-2.228588811
C,1.7973742147,-2.9064231774,1.1637282118
H,2.9538777156,-1.2583126364,1.933802601
C,1.1636490981,-3.4567734926,0.0464312348
H,0.7288942178,-3.2029110932,-2.0532336392
H,1.7766882932,-3.4306199207,2.1147804302
H,0.6481478231,-4.4094799343,0.1238211379
C,-4.2436994236,2.9203871238,-0.6799623642
C,-5.1465372637,3.3288773375,-1.6749718877
C,-3.8876162262,3.8364438786,0.3228380323
C,-5.6713233418,4.6224011528,-1.6733715733
H,-5.4302887305,2.6313777544,-2.4567962724
C,-4.4143387095,5.1280150383,0.3260519449
H,-3.1846446005,3.5414365879,1.0952832468
C,-5.3081079863,5.5264139666,-0.6719747373
H,-6.3602295953,4.9236976704,-2.4575488003
H,-4.1163574884,5.825515348,1.1033200296
H,-5.7123917331,6.5346948163,-0.6724323864
C,4.8610744764,1.8875490971,-0.291034252
C,-3.6064432976,-0.7419469337,-0.6991228376
C,6.1086813955,2.6651287825,-0.2937637547
C,6.1317308136,3.9748265706,0.2232736675
C,7.2935894055,2.1373532831,-0.8395551585
C,7.3011934873,4.7351455236,0.1893006965
H,5.2379620389,4.3931738707,0.6781817774
C,8.4615066161,2.898639484,-0.8664543915
H,7.291994367,1.1339741964,-1.2503702597
C,8.471658609,4.2000877228,-0.3548435689
H,7.2982517392,5.7421843276,0.5960305023
H,9.3650606123,2.4761815947,-1.2965270075
H,9.382693142,4.7906648476,-0.3797060379
C,-3.8399965092,-2.1944876761,-0.7005935554
C,-4.8626421492,-2.765158025,0.0792724066
C,-3.0247793757,-3.0477098644,-1.4680655062
C,-5.0589986415,-4.1456046677,0.0899054154
H,-5.4964557006,-2.1225556982,0.6801496033
C,-3.2229116675,-4.4293117521,-1.4532685565
H,-2.2509202098,-2.6256235901,-2.1036291354
C,-4.2410517136,-4.984321993,-0.6740850605
H,-5.8509698703,-4.5680199363,0.7015101435
H,-2.589708427,-5.0699902894,-2.0605070129
H,-4.3982885987,-6.0588585486,-0.6643713306
C,5.610936071,-0.5442928238,0.1554629676
C,6.4679950188,-0.457700074,1.2641629248
C,5.7422200037,-1.677906569,-0.6616847641
C,7.4077599464,-1.4449330007,1.5479202193
H,6.4020797685,0.4036682169,1.9230740906
C,6.6765054231,-2.6752631013,-0.3937027153
H,5.1079041887,-1.7810560608,-1.5373132949

C,7.530814687,-2.5942144998,0.7312674639
H,8.0411914513,-1.3157599708,2.4167138725
H,6.733095247,-3.5198810072,-1.0690631878
C,-5.9728597225,0.2636884827,-0.7136422077
C,-6.6546612721,-0.4446825572,-1.7151420563
C,-6.756482659,0.8999619514,0.2616868474
C,-8.0444912793,-0.5279230573,-1.7427725473
H,-6.0878228048,-0.9350533897,-2.501744967
C,-8.1465268857,0.8265326022,0.2504511512
H,-6.2705358524,1.4727074168,1.0459099168
C,-8.8335626792,0.0966617441,-0.7482476447
H,-8.5101749554,-1.0802302673,-2.5494023978
H,-8.6936378356,1.3466665306,1.0265672787
N,-10.2221499085,-0.0121475555,-0.7446115425
N,8.4384891719,-3.6055231702,1.0303324895
C,-10.8923678984,-0.5356337581,-1.9251533658
H,-11.9658805428,-0.5801930534,-1.7339467254
H,-10.7253743855,0.0825446463,-2.8226502318
H,-10.5570698086,-1.5544274164,-2.1458004554
C,-10.9961384231,0.8582736433,0.1282032736
H,-12.0548601158,0.6151038631,0.0235711637
H,-10.7265146192,0.6998422487,1.1775187269
H,-10.8605504229,1.9274676354,-0.102945974
C,9.45618421,-3.3686206177,2.0426572134
H,10.0524442498,-4.2741606197,2.1657952761
H,10.1346045682,-2.5395590337,1.7826044258
H,8.9990880128,-3.1432171728,3.0120280303
C,8.7073629705,-4.6330875385,0.0361858908
H,9.4150601823,-5.3526174479,0.4510137636
H,7.7939690178,-5.1813695061,-0.2179410101
H,9.1332555376,-4.2261044081,-0.8955804307

Cartesian Coordination of 3a-3

-2563.6840633 hartree
H,-1.8521316773,1.4868696726,-1.1349057002
H,1.7530439629,1.6009083444,0.4150845134
O,-1.2193908441,-2.3377442179,-0.1573657383
O,1.2290629572,-2.3319412099,-0.0537170765
F,-0.0089103088,-4.2811428786,0.3333180699
F,0.0761414807,-3.3968443173,-1.799223412
C,-1.2109975557,-1.0394523001,-0.2788665455
C,4.6673745072,0.3010737372,0.1432017554
C,-2.4936008906,-0.3789345616,-0.3493274924
C,-4.6698971763,0.3058048517,-0.2278404585
C,0.0053514574,-0.3350377611,-0.3104706841
C,1.2134266741,-1.0308346415,-0.1362136021
C,2.4849214358,-0.3568243057,0.0008982963
B,0.0221420885,-3.1467603058,-0.4317907745
N,-2.5776471878,0.9708142598,-0.6604516609
N,2.548267781,0.9973456234,0.2797181241
C,-3.7987938493,-0.8168042473,-0.0587112041
C,3.8107947501,-0.819987007,-0.0861822232
H,0.0082229826,0.7417299924,-0.4001014909
C,4.2648688588,-2.2028513808,-0.3671676244
C,3.8592054059,-2.8826466302,-1.5265576953
C,5.1371064848,-2.850181485,0.5228813548
C,4.3086988922,-4.17757376,-1.785686778
H,3.1781384584,-2.4016200295,-2.2214012188
C,5.5847751392,-4.1467189759,0.26479456
H,5.4577640799,-2.3369668657,1.4240865181

C,5.1735551701,-4.8145961833,-0.8913943903
H,3.9731186849,-4.6913471836,-2.681694502
H,6.2512027503,-4.635306308,0.9700312689
H,5.5177228013,-5.8254299757,-1.090782578
C,-4.225415941,-2.1527815968,0.4264337747
C,-4.8714549846,-2.2707622619,1.6682936306
C,-4.035322941,-3.3088627236,-0.3467943718
C,-5.3058484959,-3.5142156662,2.1302914015
H,-5.0287588342,-1.3839798976,2.2746709283
C,-4.4764463878,-4.5504950293,0.1119998272
H,-3.5279668431,-3.2359645921,-1.3026715984
C,-5.1116953492,-4.6583309476,1.3522331353
H,-5.794047432,-3.5879948918,3.0980299802
H,-4.3110085944,-5.435225141,-0.4956914042
H,-5.4469750799,-5.627108357,1.7115634254
C,3.8453610739,1.4170349941,0.3702202099
C,-3.8801360154,1.3915329586,-0.634725346
C,4.1501559715,2.8304849514,0.6414920811
C,3.3762900855,3.5640991626,1.5610934822
C,5.1930120819,3.4899182362,-0.0349064522
C,3.6312964782,4.9172685434,1.7912303118
H,2.5931294139,3.065808104,2.1271620637
C,5.4469235299,4.8406861352,0.2002038747
H,5.7959770728,2.9403757175,-0.7492404524
C,4.6677729703,5.5614260999,1.1111404151
H,3.0283823789,5.4629949021,2.5113739884
H,6.2529430107,5.3339873045,-0.3352855485
H,4.8694954731,6.6131253113,1.2915882576
C,-4.2205229112,2.7640795263,-1.0361566341
C,-5.3794111336,3.0369105379,-1.7866106039
C,-3.3663402881,3.8341987422,-0.7066129898
C,-5.6697103493,4.3386152006,-2.1927493225
H,-6.0449817428,2.223961932,-2.0546167407
C,-3.6579253563,5.1353252086,-1.1191743397
H,-2.4862243846,3.6512810801,-0.0956176556
C,-4.8114156658,5.3930434098,-1.8640258475
H,-6.5664543411,4.5290002397,-2.7752021964
H,-2.9896505166,5.947883577,-0.8488597159
H,-5.0411393387,6.4051837437,-2.1835254414
C,6.1480766748,0.2961720309,0.1560495295
C,6.8743192706,0.7912243606,1.2503683075
C,6.8895954188,-0.1995818695,-0.9280449352
C,8.2666171439,0.7962143894,1.2693075483
H,6.3408239195,1.182472566,2.1122154622
C,8.2814856869,-0.2026035183,-0.9265177542
H,6.3683986362,-0.5910011036,-1.7966051932
C,9.0138435276,0.2841278918,0.1823182511
H,8.7673315474,1.1939320647,2.1432114589
H,8.7945262112,-0.5931975422,-1.7963732108
C,-6.1299650905,0.3363401518,0.0110302077
C,-6.7146015803,1.2940572219,0.8543521805
C,-6.9924127549,-0.5969372781,-0.5860446489
C,-8.0871444867,1.3336141475,1.0847669395
H,-6.0815345589,2.0218063737,1.3545357066
C,-8.3668079486,-0.5715408941,-0.3681736542
H,-6.5818718821,-1.3647595366,-1.2347586998
C,-8.9587978062,0.4065145318,0.4658685653
H,-8.473898631,2.0900462902,1.7562662009
H,-8.9764825876,-1.3232298253,-0.8536587834
N,-10.3361107201,0.4612612611,0.6585596733

N,10.404747868,0.2442506378,0.2100676901
C,-10.8699336132,1.3144945519,1.7090230795
H,-11.9597000614,1.2601364142,1.6919170164
H,-10.5240375763,1.0236664356,2.7145715689
H,-10.591742601,2.3604972639,1.5421272308
C,-11.1561433688,-0.6616323242,0.2281915217
H,-12.2038417869,-0.4348811341,0.4323443932
H,-11.0609685132,-0.8253041304,-0.8503172301
H,-10.8976669743,-1.6017540991,0.7419647842
C,11.1148601487,0.9879664836,1.2389611273
H,12.1867383524,0.8182708124,1.1245486739
H,10.9282551785,2.0734006065,1.1882284921
H,10.8340944446,0.6406708899,2.2388974361
C,11.129396741,-0.0678709659,-1.0122345415
H,12.1981827984,-0.0979585785,-0.79397676
H,10.845217004,-1.0538961266,-1.393970497
H,10.9595240423,0.6716730857,-1.8121298753

Cartesian Coordination of 3a·Cl⁻

-3024.0287723 hartree
H,-1.76698825,1.7177796,-0.11564602
H,1.79552428,1.68795671,-0.15174397
O,-1.24569871,-2.27857933,0.18894848
O,1.19900224,-2.29699082,0.21202634
F,-0.04399616,-4.17198642,0.85911736
F,-0.0178021,-3.55111286,-1.36386167
C,-1.21665841,-0.99556583,-0.08805074
C,4.68222133,0.22972571,-0.02588288
C,-2.48980847,-0.30845687,-0.10669865
C,-4.68055649,0.30985103,-0.05841298
C,-0.00363264,-0.33524241,-0.30706983
C,1.19560742,-1.01474951,-0.07016285
C,0.248054482,-0.35047767,-0.08006426
B,-0.02741776,-3.12006566,-0.03116881
N,-2.57325516,1.07159209,-0.11671043
N,2.58940083,1.02669096,-0.13676757
C,-3.8055815,-0.81266146,-0.07404532
C,3.78622668,-0.87649501,-0.01166304
C,4.19131657,-2.30158941,0.06603541
C,3.84250731,-3.21624811,-0.94118076
C,4.97043457,-2.7581861,1.14137075
C,4.25751475,-4.54640516,-0.87333239
H,3.22590761,-2.88589227,-1.77087429
C,5.38586005,-4.0895601,1.21124811
H,5.24424245,-2.06396207,1.92988508
C,5.03308106,-4.98929492,0.20241261
H,3.96172027,-5.2397034,-1.65582861
H,5.98138744,-4.4231207,2.05718896
H,5.34989377,-6.02745624,0.25822217
C,-4.23717379,-2.23155941,-0.06484401
C,-5.0713896,-2.71408645,0.95677191
C,-3.8569673,-3.1157495,-1.0881404
C,-5.5082361,-4.04041654,0.95959821
H,-5.37015168,-2.0452766,1.75793472
C,-4.2930134,-4.44077387,-1.08704509
H,-3.19983681,-2.76623106,-1.87783339
C,-5.12238726,-4.90965932,-0.06381811
H,-6.14525903,-4.39453311,1.76609027
H,-3.97176681,-5.11012763,-1.88026117
H,-5.45531408,-5.94426471,-0.05939186

C,3.8995493,1.40104233,-0.1148158
C,-3.87683679,1.46926793,-0.09369269
C,4.30071411,2.81555947,-0.2162357
C,3.5028123,3.83641727,0.33464782
C,5.47922729,3.18070851,-0.89688863
C,3.88092469,5.17465273,0.21623036
H,2.56876412,3.59333935,0.83084308
C,5.85538949,4.51897997,-1.00608001
H,6.09490782,2.41242892,-1.35040177
C,5.0601673,5.52431689,-0.44652829
H,3.24055353,5.9435327,0.63899938
H,6.76645639,4.7764691,-1.540162
H,5.35095255,6.56770245,-0.53691983
C,-4.25281003,2.89345888,-0.13218385
C,-5.43540194,3.3085845,-0.77623569
C,-3.42796576,3.87580438,0.44877395
C,-5.78921715,4.65668516,-0.82054996
H,-6.07272513,2.57216762,-1.25170834
C,-3.78349644,5.22415108,0.39468042
H,-2.49085933,3.59582037,0.9188051
C,-4.96694176,5.62280895,-0.23203857
H,-6.70455477,4.95263825,-1.32660989
H,-3.12244675,5.96264129,0.83925058
H,-5.24038502,6.67400532,-0.27210297
C,6.15849852,0.15509712,0.07128598
C,6.86717518,0.8644117,1.05397509
C,6.9175257,-0.63606826,-0.80470009
C,8.25491653,0.79756715,1.15822726
H,6.32048364,1.49139203,1.75240063
C,8.30603537,-0.71739985,-0.71250129
H,6.41213677,-1.20135762,-1.58181038
C,9.01515564,-0.00979089,0.28293715
H,8.73788703,1.37592893,1.93648989
H,8.82932208,-1.34375595,-1.424519
C,-6.15980389,0.25767725,0.01638679
C,-6.86296208,0.86752153,1.06685235
C,-6.92407919,-0.4273313,-0.94028723
C,-8.25242035,0.81220776,1.15684449
H,-6.30918999,1.39517654,1.8382223
C,-8.31444685,-0.49394043,-0.86534
H,-6.42020064,-0.92823369,-1.76151024
C,-9.02081604,0.13780166,0.18188812
H,-8.73079076,1.2999648,1.99732461
H,-8.84216849,-1.04676706,-1.63273943
N,-10.42307092,0.11322375,0.24120563
N,10.40811838,-0.12226419,0.41360031
C,-11.06586274,0.46950438,1.49619329
H,-12.14935638,0.42269454,1.36586264
H,-10.78612573,-0.19718616,2.33045988
H,-10.81624978,1.49534105,1.7842561
C,-11.13056884,-0.85088079,-0.58671656
H,-12.205437,-0.72199753,-0.44116213
H,-10.9222344,-0.67920925,-1.64730069
H,-10.86940431,-1.89742654,-0.35256815
C,11.11063013,0.88196974,1.19655707
H,12.1753765,0.63872584,1.21235424
H,10.99206722,1.90372567,0.79578532
H,10.7615574,0.88291149,2.23371845
C,11.15781004,-0.71749276,-0.68075137
H,12.21355289,-0.76350045,-0.40411723

H,10.82447917,-1.74292879,-0.8672622
H,11.06956851,-0.15250102,-1.62532999
H,0.00565689,0.71892435,-0.54305522
Cl,0.02768656,3.07459429,0.0250855

Cartesian Coordination of 3b-1

-1796.7117483 hartree
H,-3.5171254369,3.5185703511,0.0004197812
H,3.5410002671,3.4672479907,-0.2578695381
O,-1.2059323154,3.5888469361,-0.0026685874
O,1.2369205662,3.5709076781,-0.0945223475
F,0.0082359002,5.4920791888,-0.6169853382
F,0.0850169714,4.7631387416,1.5700454314
C,-1.198038814,2.2744537633,0.1034166409
C,4.394856827,0.3710042558,-0.1893449633
C,-2.5041648133,1.6788549196,0.1267439247
C,-4.4088715671,0.4370494192,0.173744369
C,0.0080900882,1.5639336855,0.1489716694
C,1.2173564282,2.2565181739,0.0090881328
C,2.5121472276,1.6414256967,-0.0725312586
B,0.0319063409,4.4050437987,0.228453154
N,-3.6071700451,2.5139932475,0.0677389974
N,3.6202565856,2.4607541949,-0.2078480819
C,-2.98701114,0.3593158942,0.197000742
C,2.9780661694,0.3141377476,-0.0556891833
H,0.0032174648,0.4916493532,0.2271728335
C,4.7576633534,1.7250665766,-0.2811542731
C,-4.7575823688,1.7955919209,0.0928475367
C,5.3307428265,-0.7753921574,-0.2333445287
C,6.3753820348,-0.9152240997,0.6946102274
C,5.2230938809,-1.7728667624,-1.2165823518
C,7.2647332217,-1.98703112,0.6520197653
H,6.4926641739,-0.1717437037,1.478688179
C,6.0976475133,-2.8551456674,-1.2717723034
H,4.4462571116,-1.6914108341,-1.9722241514
C,7.1404984507,-3.0012968134,-0.3263520982
H,8.05080791,-2.0341648043,1.3953899722
H,5.9655142277,-3.5836441576,-2.0619920253
C,-5.3639251893,-0.6931789677,0.2226858987
C,-6.3286122674,-0.8024043652,1.2373140899
C,-5.3459880451,-1.71338157,-0.7426823075
C,-7.2332439436,-1.8608911962,1.2878470865
H,-6.3621088097,-0.0504602849,2.0213710859
C,-6.2367938676,-2.7831996037,-0.7053039822
H,-4.622330831,-1.6658106624,-1.5520672084
C,-7.2198478708,-2.8810766056,0.3078622256
H,-7.9454407709,-1.8913308141,2.1030127449
H,-6.1672061963,-3.5379725378,-1.4786874246
N,-8.1400093533,-3.9257465142,0.3303016335
N,7.9942120406,-4.1005540831,-0.3488214782
C,-8.9620552566,-4.1188543594,1.5152239096
H,-9.640913726,-4.9559100775,1.3441960851
H,-8.3682031749,-4.3331125648,2.4189921662
H,-9.5767032066,-3.2343839591,1.7129687718
C,-7.9165662224,-5.082093847,-0.5242177448
H,-8.741164753,-5.7848537389,-0.3943015388
H,-7.8979738063,-4.7919852057,-1.5799884004
H,-6.9744279614,-5.6070979814,-0.2959891509
C,9.1979451794,-4.0793292318,0.468264483
H,9.7274614352,-5.0255625954,0.3456875963

H,9.8844477747,-3.2602766374,0.1979211433
H,8.9488152147,-3.9789831209,1.5299620438
C,7.9865199434,-4.9788523438,-1.508444998
H,8.6840282936,-5.8004000062,-1.3372840422
H,6.99487133,-5.4182988526,-1.6595843929
H,8.2790708572,-4.4638847236,-2.4382446099
C,-2.1821358631,-0.900900433,0.3246408415
H,-1.5654552004,-1.0887972508,-0.5632595076
H,-1.5090506821,-0.8628946693,1.1891141892
H,-2.8415695833,-1.7611710121,0.4574304958
C,2.165831962,-0.9358426094,0.1176018833
H,1.5687606282,-0.9039916846,1.036520453
H,1.4734497662,-1.0973331074,-0.7180948159
H,2.8196056735,-1.8083928149,0.1791619648
C,6.0996805884,2.3622474609,-0.4482742319
H,6.4604303036,2.8056531086,0.4886394936
H,6.83253679,1.6186970857,-0.7682726938
H,6.0691422551,3.1594045081,-1.1998412549
C,-6.0991517738,2.4514211671,0.0223058997
H,-6.8648277888,1.7161127999,-0.2334874555
H,-6.3808773046,2.9084001625,0.9795651914
H,-6.1147051384,3.2413655151,-0.7372642144

Cartesian Coordination of 3b-2

-1796.7059504 hartree

H,-1.8409093688,-0.6179878665,-0.1824869869
H,3.4904763774,3.4004305883,0.2654502889
O,-1.2629395614,3.3743505517,0.2058972234
O,1.1820403828,3.4250958841,0.2797299595
F,-0.0719787892,5.3793661863,0.0091309084
F,-0.1136058529,4.284709859,2.0404206071
C,-1.2233872885,2.068268532,0.109937555
C,4.4461168998,0.3518522623,-0.0664561396
C,-2.4900037283,1.4151237097,-0.0610009936
C,-4.6840430227,0.8489155695,-0.285805806
C,0.0050619648,1.3827948964,0.1436189371
C,1.1982025079,2.1103664409,0.1886470825
C,2.5166963367,1.543324643,0.1050520061
B,-0.0703310038,4.1653923972,0.6567621226
N,-2.6065897913,0.0363408149,-0.2081941425
N,3.6019887333,2.4000854258,0.1712775436
C,-3.7901106024,1.9461561414,-0.1127781655
C,3.0258767713,0.2414329137,-0.0429415607
H,0.0437512539,0.3081721873,0.069189741
C,4.7670996396,1.7120590247,0.0700123802
C,-3.9139516373,-0.3203245464,-0.3384669083
C,5.4224709576,-0.7521542578,-0.2102952667
C,6.3909715917,-1.014559287,0.7720634092
C,5.4340597011,-1.5812120062,-1.3440759166
C,7.3198869091,-2.0445089942,0.6393536232
H,6.4158169227,-0.4033026727,1.6704362383
C,6.350202048,-2.6197483644,-1.4923243796
H,4.7202243605,-1.3980277676,-2.1429782844
C,7.3160250208,-2.890791563,-0.4943257917
H,8.0425174954,-2.1903994442,1.4326794932
H,6.311520288,-3.2137067528,-2.3970219363
C,-6.1597250655,0.9051530407,-0.3876457215
C,-6.8425123261,0.3922997061,-1.5021033115
C,-6.9455322037,1.4760602673,0.6270083428
C,-8.2317730461,0.4313962496,-1.6015392741

H,-6.2736848897,-0.0306699102,-2.3261283091
C,-8.3343733961,1.5294527581,0.5433936286
H,-6.4599505843,1.884703938,1.5089362926
C,-9.0217721359,0.9928815912,-0.5712098993
H,-8.6955338978,0.0289062388,-2.4934726703
H,-8.8811782759,1.9873696436,1.3581425947
N,-10.4121911807,1.0049141846,-0.6429852078
N,8.2110124627,-3.9502441079,-0.6154371156
C,-11.0578407019,0.6765385066,-1.904625028
H,-12.1401196072,0.7019289989,-1.767334203
H,-10.794996969,1.3751637662,-2.7159641776
H,-10.7926851686,-0.3358342929,-2.2273863089
C,-11.1613830343,1.8240673578,0.2980908653
H,-12.2285823792,1.6936223941,0.1114363931
H,-10.9693453714,1.510722682,1.3296480451
H,-10.9231244997,2.8970169579,0.2152120545
C,9.3460032058,-4.0245361926,0.2921045961
H,9.9213720762,-4.9243349754,0.0685767189
H,10.0171459245,-3.1539717201,0.2096474381
H,9.0122072714,-4.1002027416,1.3323506509
C,8.3339945324,-4.629983843,-1.8958259654
H,9.0457495051,-5.451002973,-1.7953710096
H,7.3760618122,-5.0633111085,-2.2020654474
H,8.6832982711,-3.9651876416,-2.7029938229
C,-4.1723981306,3.394950802,-0.038445933
H,-3.9691605428,3.8127531766,0.9537445313
H,-3.592618874,3.9939184889,-0.7453931243
H,-5.2355284897,3.5191616391,-0.2558765654
C,2.2501073094,-1.0418680723,-0.1154771579
H,1.5986711865,-1.1684786095,0.7576573288
H,1.6192339789,-1.0926059938,-1.0121954365
H,2.9309343792,-1.8953966801,-0.1426819787
C,6.0944437013,2.3996587882,0.093015101
H,6.3656744493,2.7302248992,1.1037584045
H,6.8753558851,1.7213426434,-0.2566325388
H,6.094258906,3.2843841985,-0.5540509663
C,-4.3252933466,-1.75044288,-0.4820460808
H,-5.3935565601,-1.8539800105,-0.2813129001
H,-4.1383776541,-2.1323689216,-1.4940870336
H,-3.7828077516,-2.3942371781,0.2205295004

Cartesian Coordination of 3b-3

-1796.6988676 hartree

H,-1.9381108865,-0.7290658577,0.0909154808
H,1.899405628,-0.7568088749,0.0311905278
O,-1.2178092796,3.2525398879,-0.2055467396
O,1.2294745427,3.2357611747,-0.2311905448
F,0.0134983112,5.168419271,-0.7353574953
F,0.0309270937,4.3778791475,1.4337439541
C,-1.2166545489,1.9477400784,-0.0934071872
C,4.7054381226,0.7457062572,-0.2922125371
C,-2.509927079,1.320823492,-0.1167737257
C,-4.7283112954,0.8106255279,-0.1900906604
C,-0.005558846,1.2420587978,0.0063498306
C,1.2127011272,1.9310308383,-0.1198866618
C,2.4962819618,1.286314007,-0.1727114092
B,0.0145929996,4.0622231179,0.080856599
N,-2.6787722298,-0.0579729881,-0.0323897347
N,2.647371392,-0.0951102289,-0.0985459683
C,-3.7910138556,1.8861070678,-0.2235071174

C,3.7828501289,1.8343120409,-0.3015330883
H,-0.0120016092,0.1650500381,0.1032013622
C,3.9653407405,-0.4353203645,-0.1617800458
C,-4.0024005055,-0.3799312063,-0.0675241471
C,6.1797890507,0.8268914139,-0.3950901376
C,6.8897471658,0.1503434375,-1.3997030661
C,6.9388490986,1.5789064547,0.5168651459
C,8.2783106095,0.2149732295,-1.4966683135
H,6.3442688843,-0.4341066503,-2.1362059818
C,8.3262002343,1.6600709717,0.4332894055
H,6.4338728861,2.1036564979,1.323236276
C,9.0386602049,0.9878816403,-0.5881207315
H,8.7640276405,-0.3313536789,-2.2957443563
H,8.8514205798,2.2506821657,1.1736467519
C,-6.2031246246,0.9110193902,-0.2658874663
C,-6.9393659053,0.2477240294,-1.2604273763
C,-6.9346864972,1.6827633375,0.6518586438
C,-8.3278809265,0.3359748494,-1.3365307485
H,-6.4139934185,-0.3363521809,-2.0117097635
C,-8.3216943489,1.7870134634,0.5892071721
H,-6.4073401861,2.2133155295,1.4398856152
C,-9.0634623381,1.1025728865,-0.4026375554
H,-8.8331808012,-0.1901716501,-2.1370024675
H,-8.8236762274,2.4033665629,1.3246714767
N,-10.4535061927,1.1702815005,-0.4486855869
N,10.4215352575,1.0950006674,-0.7025503885
C,-11.1455261787,0.677173419,-1.6296973858
H,-12.2214613853,0.7819135629,-1.480758627
H,-10.8677571525,1.2211175349,-2.5474695191
H,-10.9396594999,-0.3866458578,-1.7883546505
C,-11.1384253793,2.1712134045,0.3557773951
H,-12.2153057455,2.0625921122,0.2167303554
H,-10.9304093208,2.0264325678,1.4210331326
H,-10.856006839,3.2024612303,0.0879330073
C,11.1293788918,0.195581839,-1.6001861564
H,12.1931302118,0.4378741151,-1.5805617683
H,11.0105817222,-0.8653735936,-1.3248201115
H,10.7847714485,0.3200403318,-2.632359976
C,11.1792620197,1.6876963523,0.3889101542
H,12.2346325979,1.7187109636,0.1133351456
H,10.8591399784,2.7185255627,0.5735624557
H,11.0836146709,1.1247122348,1.3318708005
C,-4.123061715,3.3404598402,-0.3841269022
H,-3.8982578738,3.9062970997,0.5268311237
H,-3.5293649239,3.7965014513,-1.1801311049
H,-5.1833549403,3.4640799309,-0.6152587236
C,4.13220145,3.2848328775,-0.4601185257
H,3.5350326933,3.7519866843,-1.2471181406
H,3.925836196,3.8497986933,0.4556777278
H,5.1910751373,3.3954674221,-0.7038578094
C,4.4114345132,-1.8594751933,-0.0717701572
H,4.2348698635,-2.4062595383,-1.0072184939
H,5.4817840756,-1.9028601907,0.1395734453
H,3.8852593835,-2.3933019197,0.728823966
C,-4.4667034183,-1.797020349,0.0399409824
H,-5.532945282,-1.8239837992,0.2736199159
H,-4.3172325373,-2.3513883525,-0.8957431758
H,-3.9316918501,-2.3338623976,0.8326186814

-2257.0423836 hartree
H,1.70557043,-1.67920513,-0.23874976
H,-1.73034354,-1.65709804,-0.21665442
O,1.2496043,2.33188738,0.32074062
O,-1.21556215,2.34758816,0.33731058
F,0.03417589,4.15421829,1.14620425
F,0.01614253,3.72809553,-1.11891384
C,1.2151123,1.04193192,0.05086351
C,-4.63943488,-0.28630911,0.03568154
C,2.46854819,0.33693253,0.01088839
C,4.63501749,-0.34552091,-0.02572106
C,0.00127178,0.38369438,-0.14974488
C,-1.20131,1.05738609,0.06676281
C,-2.46413927,0.36859348,0.04333288
B,0.02119861,3.17437224,0.16475709
N,2.51394021,-1.04227753,-0.15095394
N,-2.52927847,-1.00982885,-0.11824608
C,3.79365043,0.79756844,0.0954814
C,-3.78203623,0.84597523,0.14564708
C,-3.81746391,-1.41932861,-0.12049552
C,3.79669388,-1.46806871,-0.17008681
C,-6.1162616,-0.29385523,0.06124964
C,-6.84283826,-1.17390179,0.88074546
C,-6.87508071,0.56923553,-0.74838253
C,-8.23724947,-1.19711346,0.89750586
H,-6.3050839,-1.85564144,1.53351449
C,-8.26890628,0.56566793,-0.73869176
H,-6.36127866,1.25060287,-1.42023575
C,-8.9926428,-0.31269045,0.0973573
H,-8.72901309,-1.90544953,1.55343821
H,-8.78616646,1.25413362,-1.39616143
C,6.11179889,-0.37451734,-0.02107055
C,6.83617798,-1.25984007,0.79503968
C,6.87257464,0.48117419,-0.83630634
C,8.22998381,-1.30279078,0.79474198
H,6.29710676,-1.92230142,1.46633325
C,8.26647471,0.45796599,-0.84350636
H,6.36056924,1.18000949,-1.49134398
C,8.98737484,-0.44973731,-0.03704046
H,8.71998385,-2.00657658,1.4568717
H,8.78571004,1.14979751,-1.49582846
N,10.3908571,-0.51785775,-0.07900373
N,-10.39718553,-0.28985819,0.14928119
C,11.07769567,-1.19977078,1.00624628
H,12.15210969,-1.18773629,0.80913815
H,10.89888197,-0.73600199,1.99232896
H,10.76930921,-2.24805603,1.06436589
C,11.11322098,0.58763277,-0.68811467
H,12.18316774,0.36853528,-0.6639181
H,10.82896448,0.70629687,-1.73813253
H,10.94301535,1.55175933,-0.17741869
C,-11.0794409,-1.41926995,0.76007306
H,-12.155992,-1.23458782,0.74367787
H,-10.88186553,-2.37616216,0.24540458
H,-10.78438886,-1.53162594,1.80785051
C,-11.11375629,0.37403279,-0.92793104
H,-12.18550813,0.33014568,-0.7209577
H,-10.83666427,1.43092655,-0.98613771
H,-10.93067441,-0.08211491,-1.91680231
C,4.2352419,2.21816468,0.30731588

Cartesian Coordination of 3b·Cl⁻

H,4.13488668,2.81532542,-0.60795693
H,3.62167862,2.71224279,1.06359467
H,5.28308148,2.25244639,0.61913081
C,-4.20293859,2.27190586,0.36352911
H,-3.57348277,2.75797913,1.11189653
H,-4.10698021,2.86809637,-0.55283618
H,-5.24611365,2.31924882,0.68893861
C,-4.16254236,-2.86661871,-0.28856898
H,-4.26152007,-3.37636921,0.6786443

H,-5.11235618,-2.97790688,-0.81991198
H,-3.37575859,-3.38433412,-0.84495575
C,4.12184035,-2.91954432,-0.34146122
H,5.06547319,-3.04261564,-0.88108221
H,4.22290619,-3.43059292,0.62484537
H,3.32370899,-3.42728617,-0.89083625
H,-0.00686616,-0.66966874,-0.38806099
Cl,-0.02384792,-3.10940321,-0.4591401

4. Anion-binding and protonation behaviors

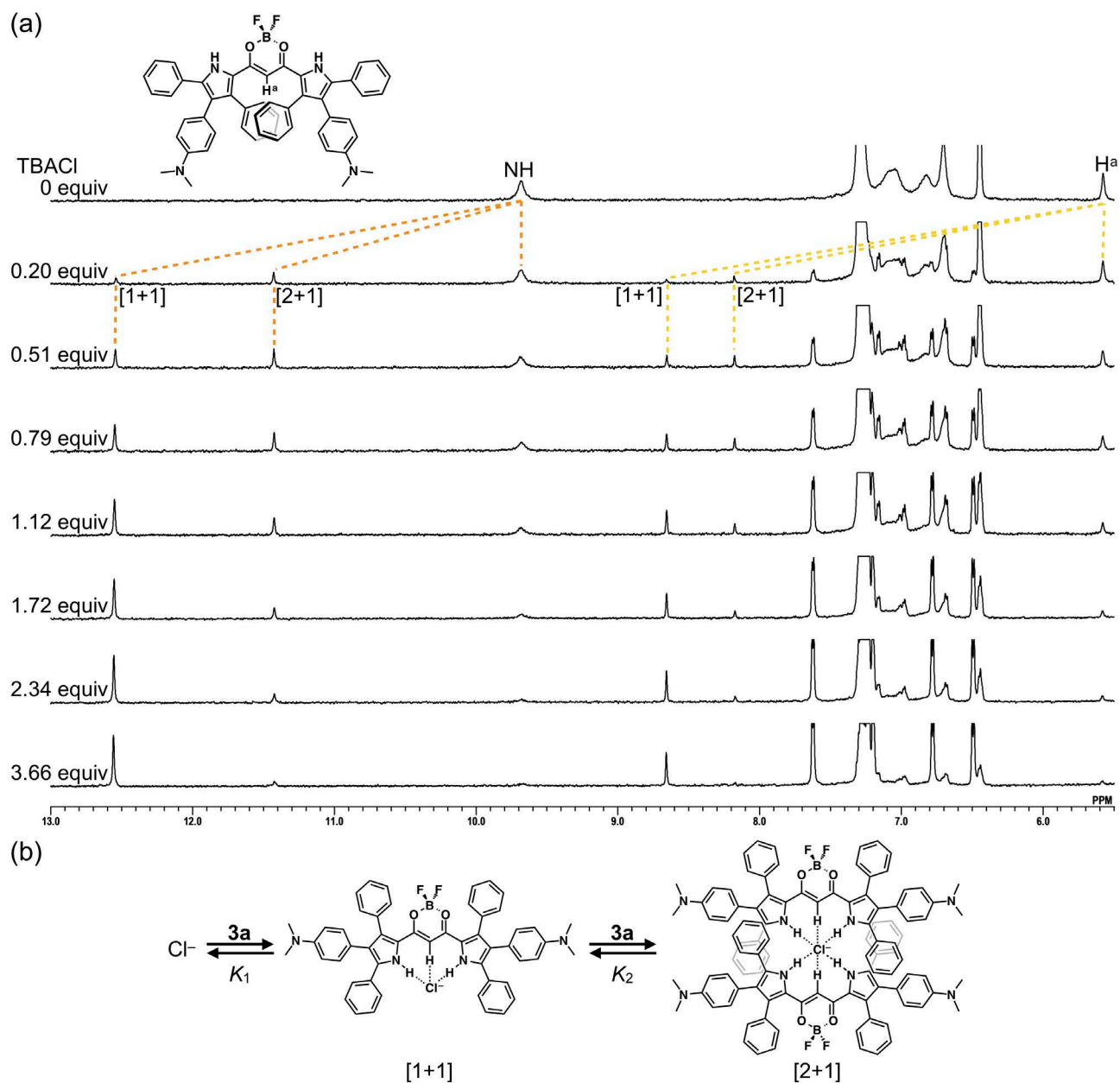


Fig. S15 (a) ^1H NMR spectral changes of **3a** (1×10^{-3} M) upon the addition of Cl^- added as a tetrabutylammonium (TBA) salt (0–3.66 equiv) in CD_2Cl_2 at -50 °C and (b) formation of [1+1] and [2+1]-type Cl^- complexes. [1+1]- and [2+1]-type binding constants (K_1 and K_2) of **3a**, estimated from the integrals of the pyrrole NH signals, were 2.7×10^3 and 1.6×10^3 M^{-1} , respectively.

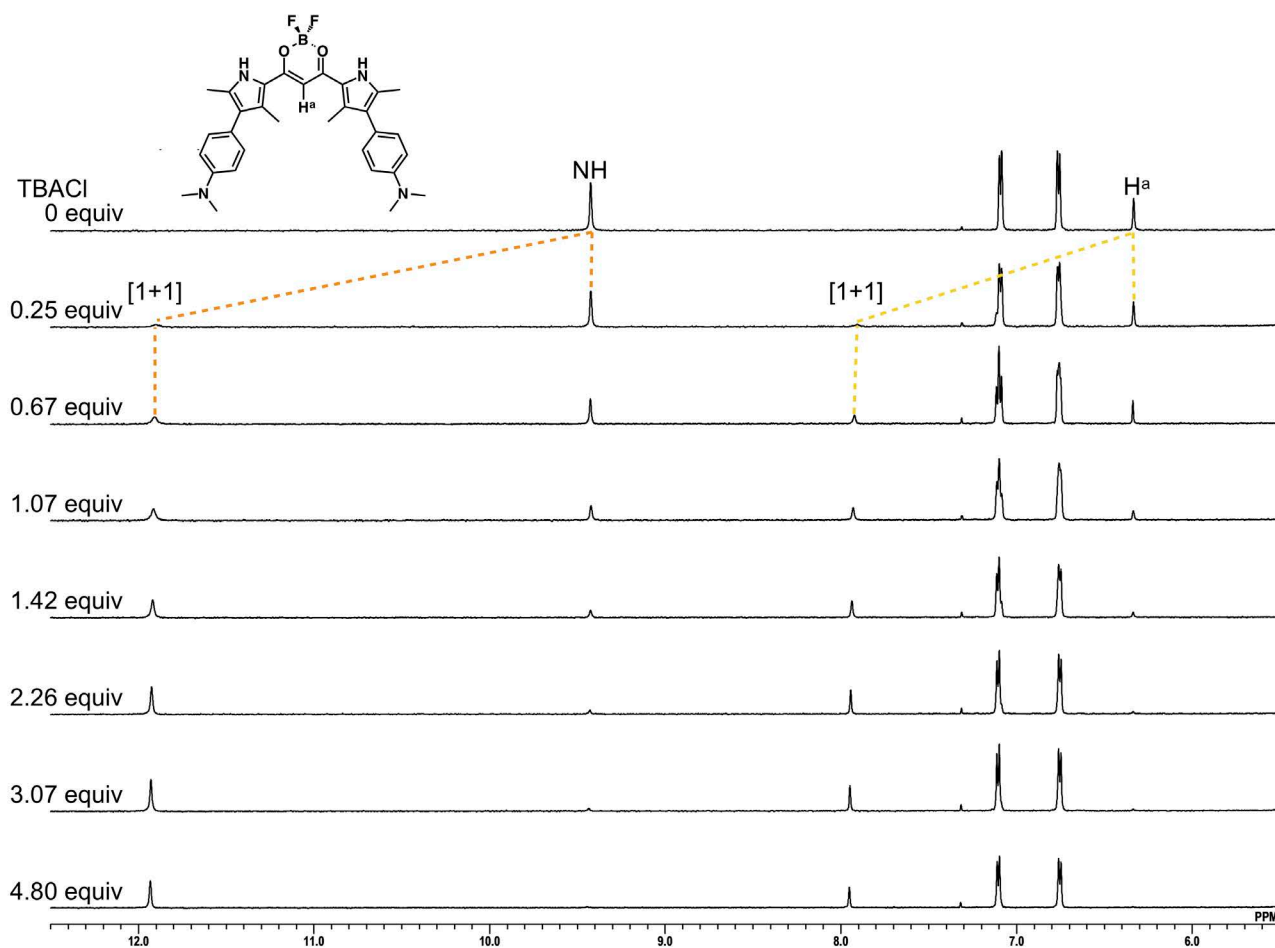


Fig. S16 ^1H NMR spectral changes of **3b** (1×10^{-3} M) upon the addition of Cl^- as a TBA salt (0–4.80 equiv) in CD_2Cl_2 at -50 °C. [1+1]-Type binding constant (K_1) of **3b**, estimated from the integrals of the pyrrole NH signals, was $3.0 \times 10^3 \text{ M}^{-1}$.

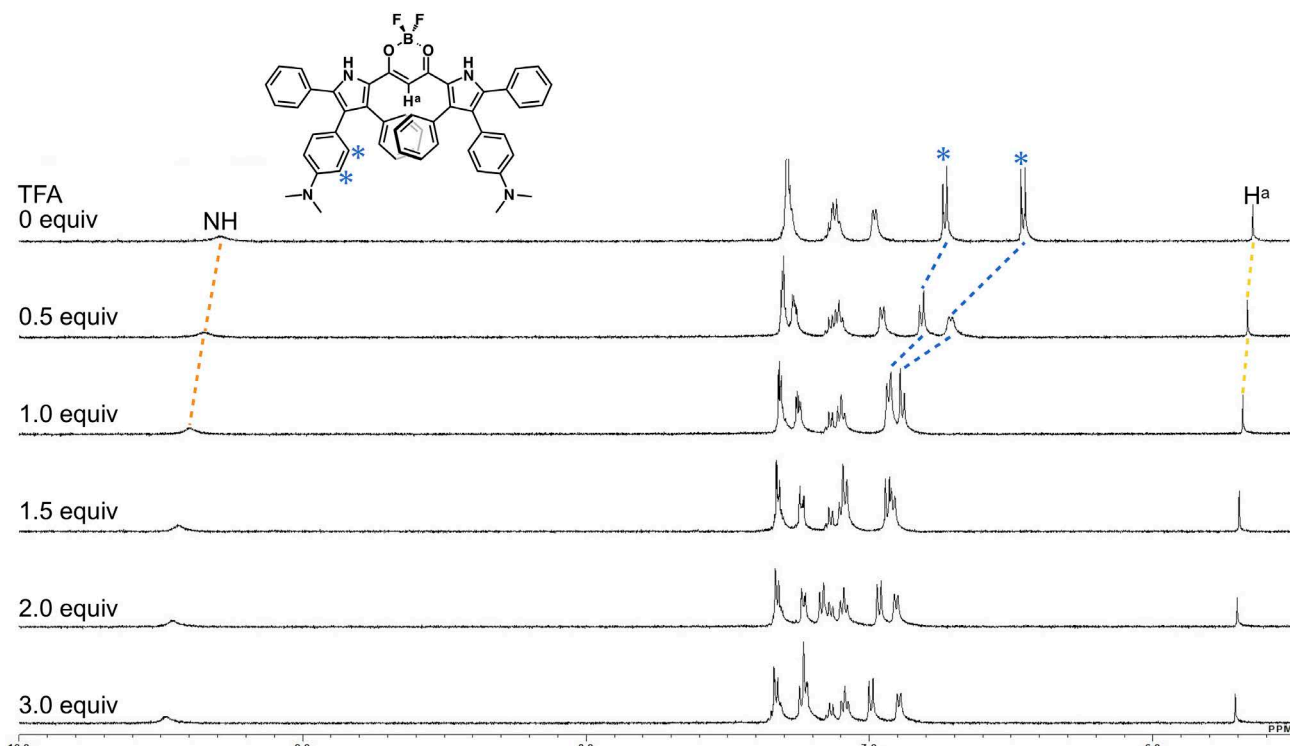


Fig. S17 ^1H NMR spectral changes of **3a** (1×10^{-3} M) upon the addition of TFA (0–3.0 equiv) in CD_2Cl_2 at 20 °C. ^1H NMR signal of TFA and *N,N*-dimethylammonium NH could not be observed. The downfield shifts of *N,N*-dimethylaminophenyl aryl-H (blue asterisks) suggested the changes to electron-deficient states by the protonation. Slight downfield shifts, including those of pyrrole NH and bridging CH (H^a), were also consistent with the protonation.

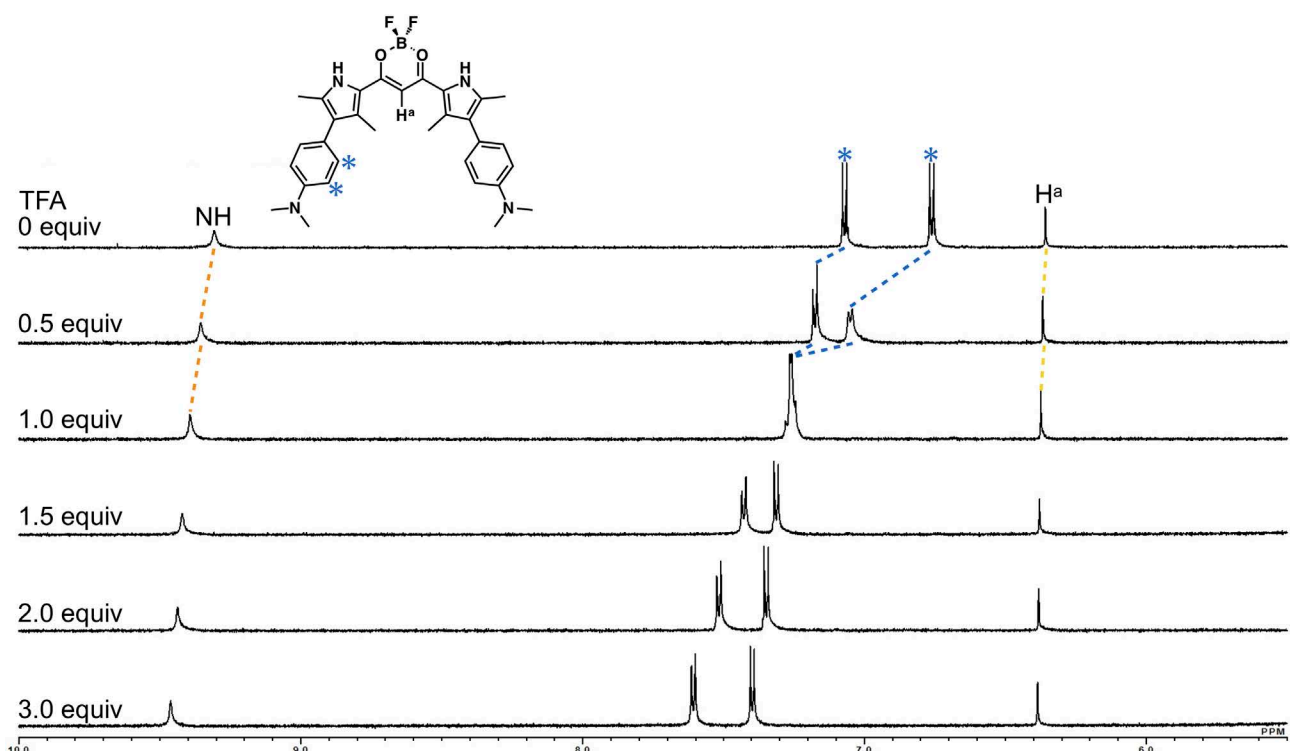


Fig. S18 ^1H NMR spectral changes of **3b** (1×10^{-3} M) upon the addition of TFA (0–3.0 equiv) in CD_2Cl_2 at 20 °C. ^1H NMR signal of TFA and *N,N*-dimethylammonium NH could not be observed. The downfield shifts of *N,N*-dimethylaminophenyl aryl-H (blue asterisks) suggested the changes to electron-deficient states by the protonation. Slight downfield shifts, including those of pyrrole NH and bridging CH (H^a), were also consistent with the protonation.

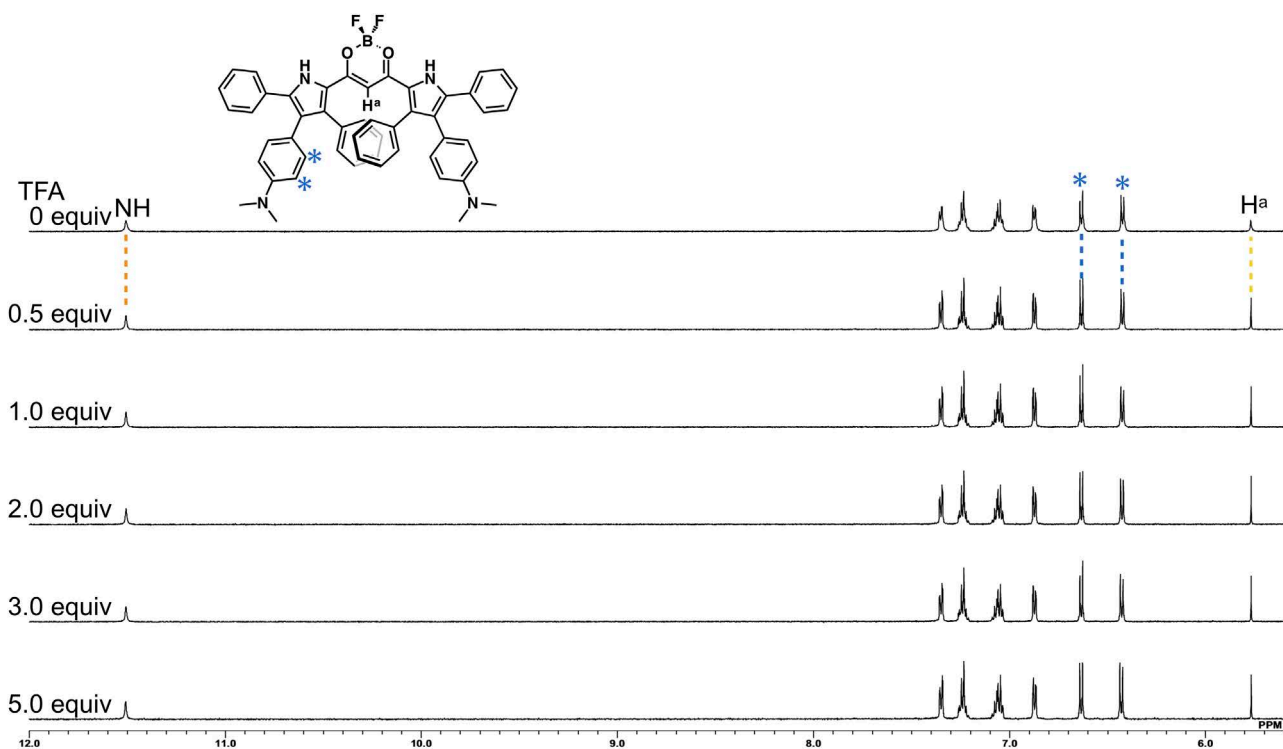


Fig. S19 ^1H NMR spectral changes of **3a** (1×10^{-3} M) upon the addition of TFA (0–5.0 equiv) in $\text{THF-}d_8$ at 20 °C. ^1H NMR signal of TFA and *N,N*-dimethylammonium NH could not be observed. No ^1H NMR signal changes of **3a** upon the addition of TFA suggested no protonation in THF.

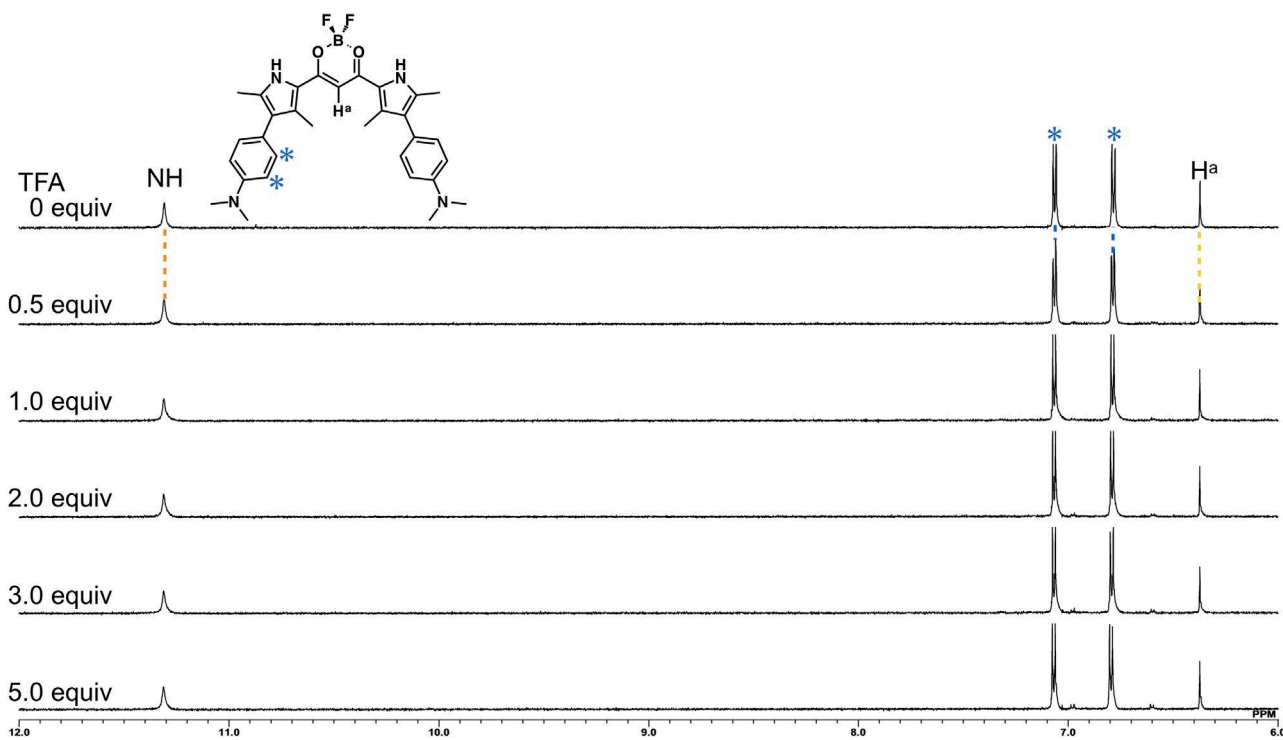


Fig. S20 ^1H NMR spectral changes of **3b** (1×10^{-3} M) upon the addition of TFA (0–5.0 equiv) in $\text{THF-}d_8$ at 20 °C. ^1H NMR signal of TFA and *N,N*-dimethylammonium NH could not be observed. No ^1H NMR signal changes of **3b** upon the addition of TFA suggested no protonation in THF.

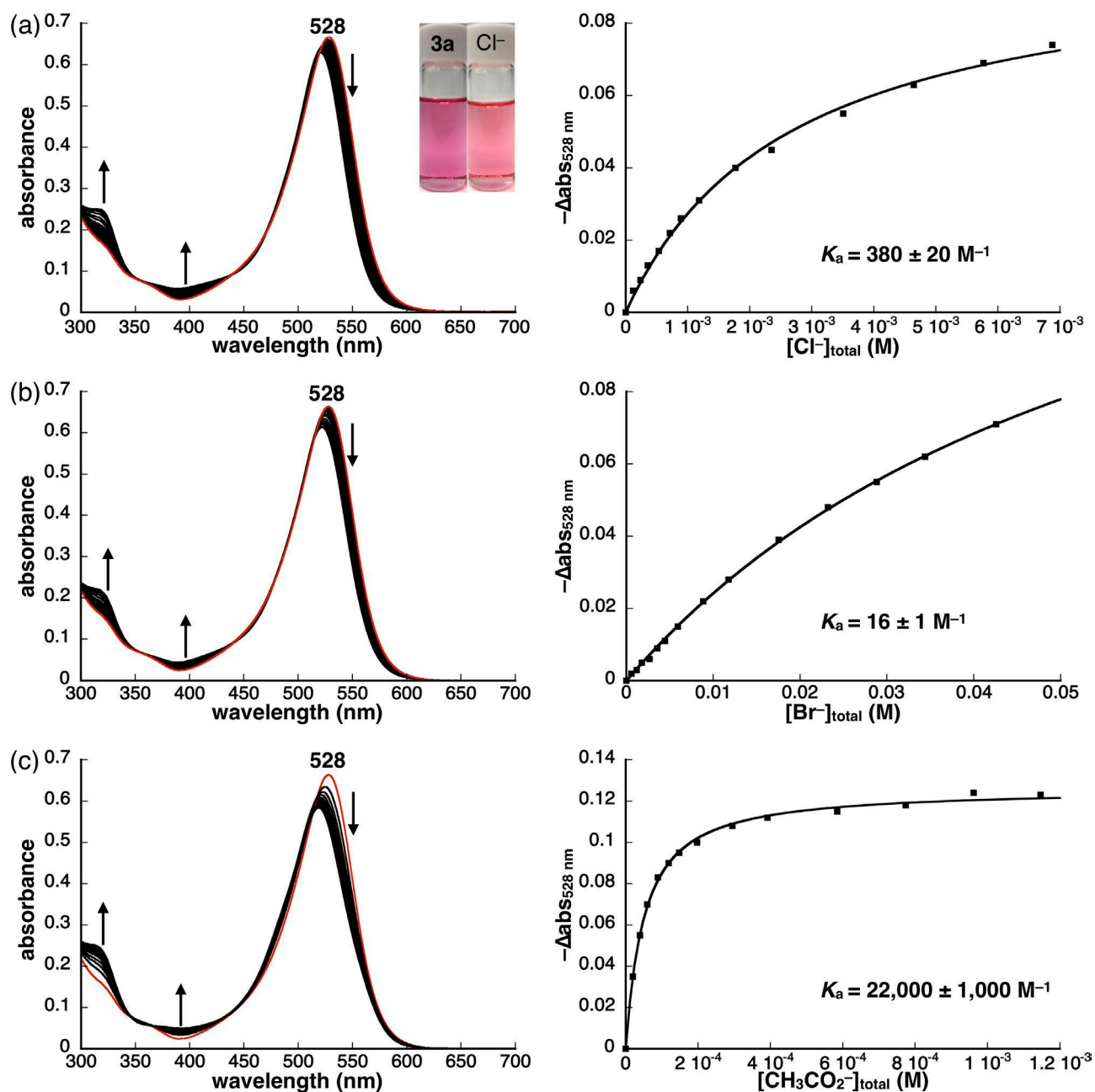


Fig. S21 UV/vis absorption spectral changes (left) and titration plots and 1:1 fitting curves (right) of **3a** (1.0×10^{-5} M) upon the addition of (a) Cl^- , (b) Br^- , and (c) CH_3CO_2^- as TBA salts in CH_2Cl_2 (red lines: initial states of **3a**) and photographs under visible light in the absence and presence of Cl^- (600 equiv) under the conditions for spectral measurements (inset).

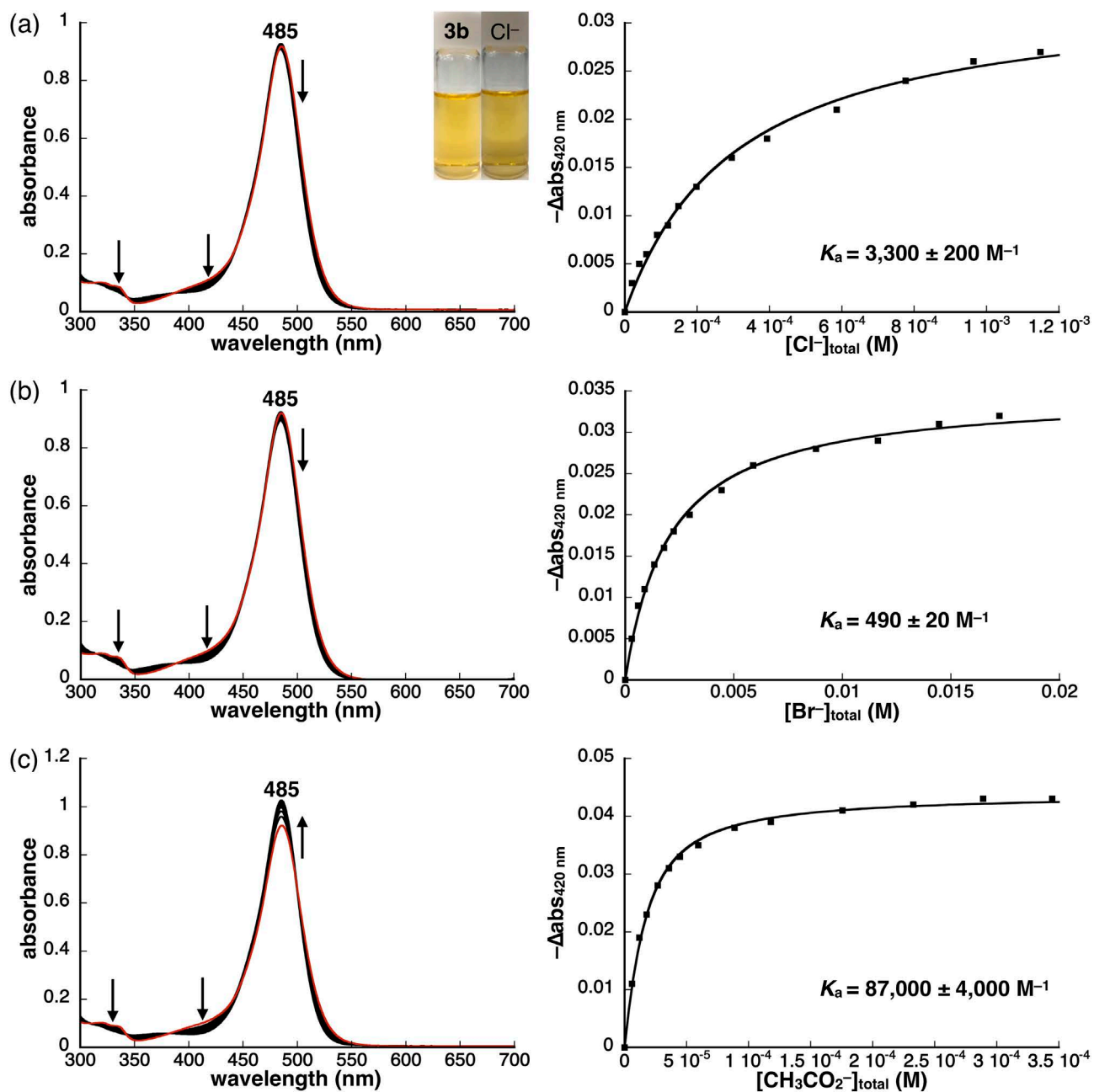


Fig. S22 UV/vis absorption spectral changes (left) and titration plots and 1:1 fitting curves (right) of **3b** (1.0×10^{-5} M) upon the addition of (a) Cl^- , (b) Br^- , and (c) CH_3CO_2^- as TBA salts in CH_2Cl_2 (red lines: initial states of **3b**) and photographs under visible light in the absence and presence of Cl^- (100 equiv) under the conditions for spectral measurements (inset).

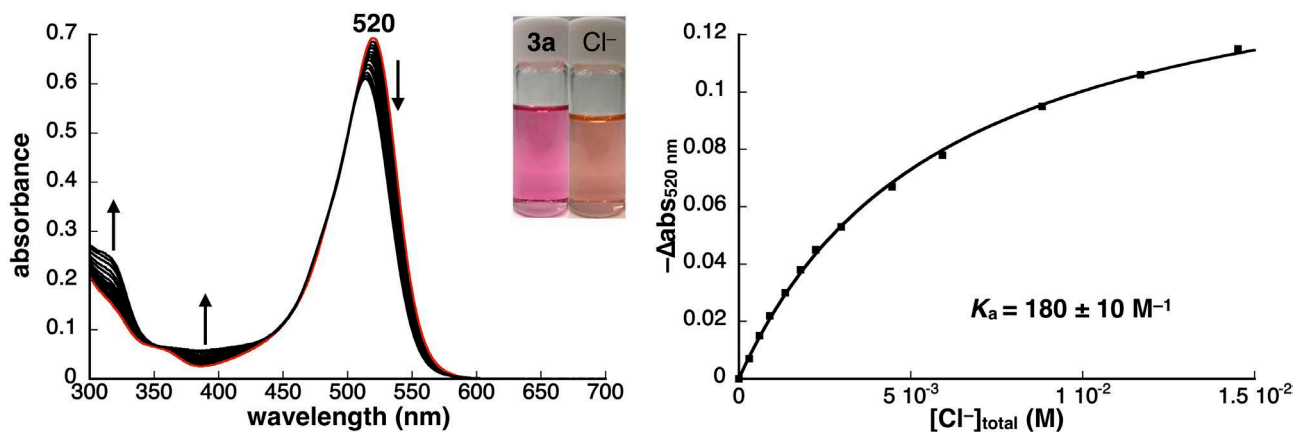


Fig. S23 UV/vis absorption spectral changes (left) and titration plots and 1:1 fitting curve (right) of **3a** (1.0×10^{-5} M) upon the addition of Cl^- as a TBA salt in THF (red lines: initial state of **3a**) and photographs under visible light in the absence and presence of Cl^- (1500 equiv) under the conditions for spectral measurements (inset). From this experiment, Cl^- , which is more effectively bound than Br^- , was examined as a representative anion for sensing by considering the previous study, in which CH_3CO_2^- induced another PET process and resulting fluorescence quenching.^[S1]

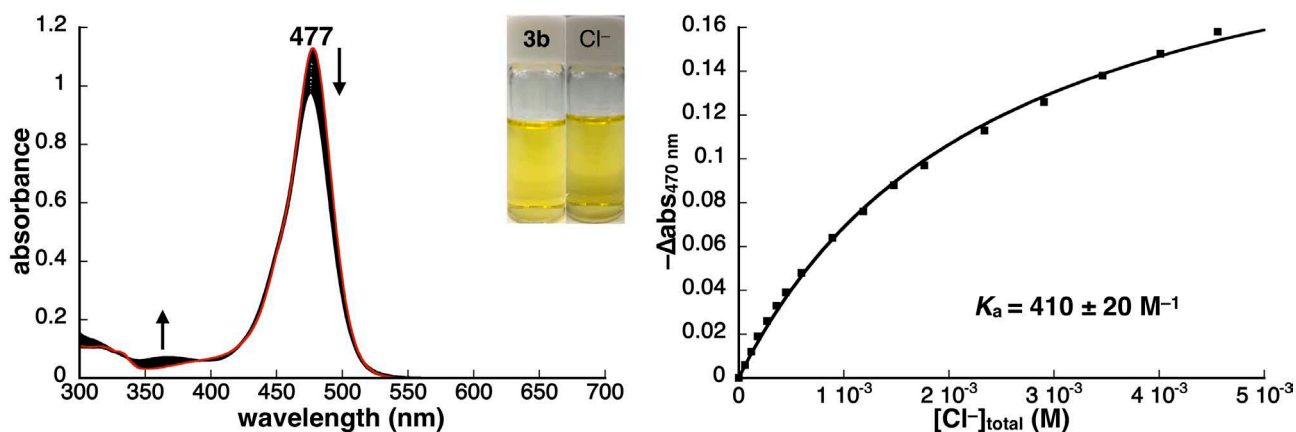


Fig. S24 UV/vis absorption spectral changes (left) and titration plots and 1:1 fitting curve (right) of **3b** (1.0×10^{-5} M) upon the addition of Cl^- as a TBA salt in THF (red lines: initial state of **3b**) and photographs under visible light in the absence and presence of Cl^- (600 equiv) under the conditions for spectral measurements (inset).

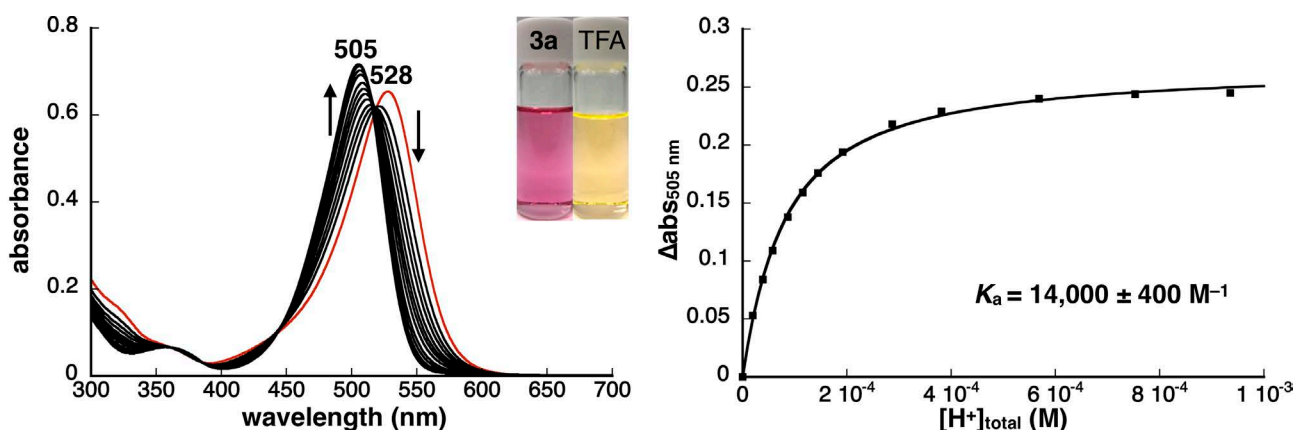


Fig. S25 UV/vis absorption spectral changes (left) and titration plots and 1:1 fitting curve (right) of **3a** (1.0×10^{-5} M) upon the addition of trifluoroacetic acid (TFA) in CH_2Cl_2 (red lines: initial state of **3a**) and photographs under visible light in the absence and presence of TFA (100 equiv) under the conditions for spectral measurements (inset). The spectral changes by protonation were fitted to the 1:1 binding curve, suggesting that protonated processes at two N,N -dimethylamino units were not cooperative. Thus, the host concentration was set to the twice of **3a**.

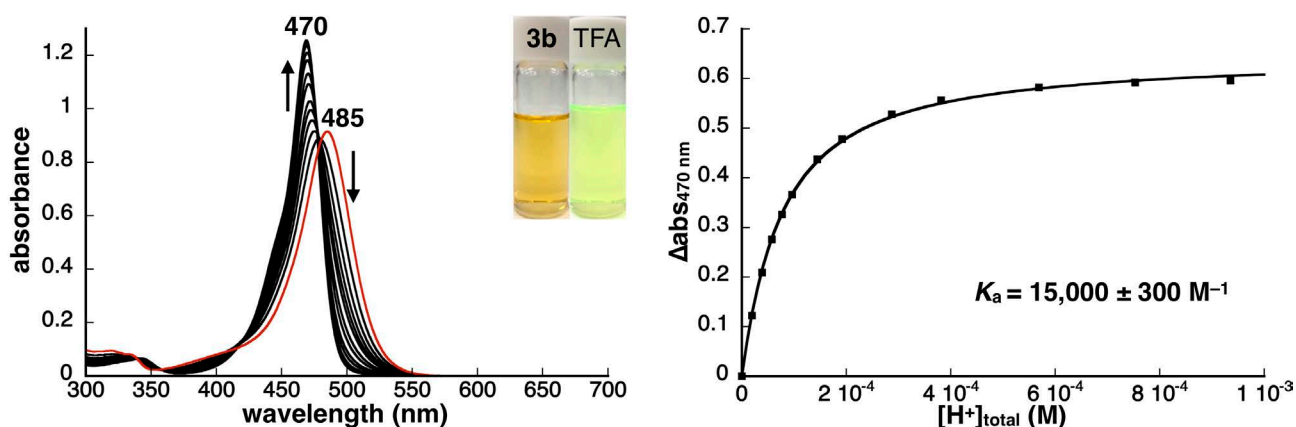


Fig. S26 UV/vis absorption spectral changes (left) and titration plots and 1:1 fitting curve (right) of **3b** (1.0×10^{-5} M) upon the addition of TFA in CH_2Cl_2 (red lines: initial state of **3b**) and photographs under visible light in the absence and presence of TFA (100 equiv) under the conditions for spectral measurements (inset). The spectral changes by protonation were fitted to the 1:1 binding curve, suggesting that protonated processes at two *N,N*-dimethylamino units were not cooperative. Thus, the host concentration was set to the twice of **3b**.

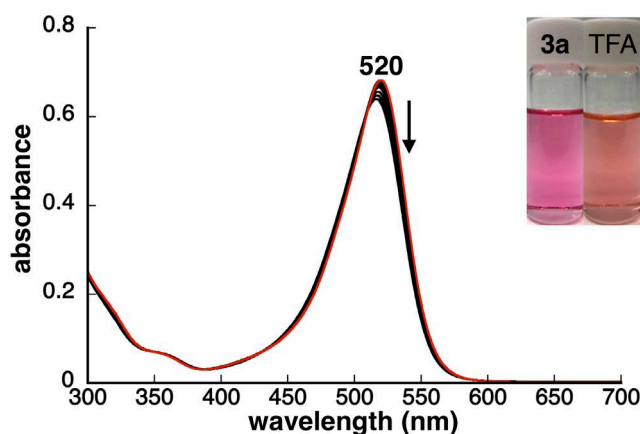


Fig. S27 UV/vis absorption spectral changes of **3a** (1.0×10^{-5} M) upon the addition of TFA (0–9000 equiv) in THF (red lines: initial state of **3a**) and photographs under visible light in the absence and presence of TFA (9000 equiv) under the conditions for spectral measurements (inset). The small spectral changes along with a very low fluorescence quantum yield (Φ_{FL} : 0.000) was observed, suggesting that **3a** showed very weak interactions with proton in THF.

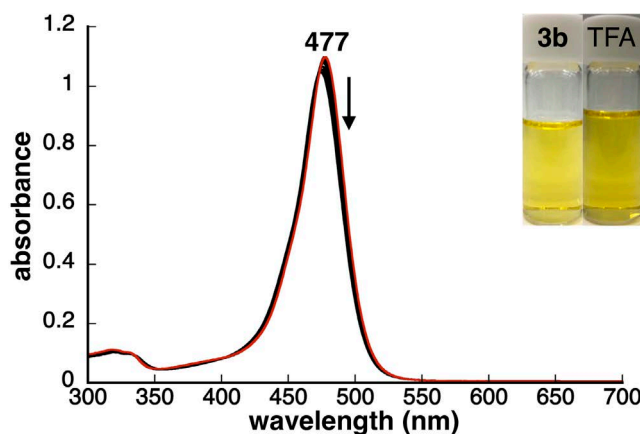


Fig. S28 UV/vis absorption spectral changes of **3b** (1.0×10^{-5} M) upon the addition of TFA (0–9000 equiv) in THF (red lines: initial state of **3b**) and photographs under visible light in the absence and presence of TFA (9000 equiv) under the conditions for spectral measurements (inset). The small spectral changes along with a very low fluorescence quantum yield (Φ_{FL} : 0.027) was observed, suggesting that **3b** showed very weak interactions with proton in THF.

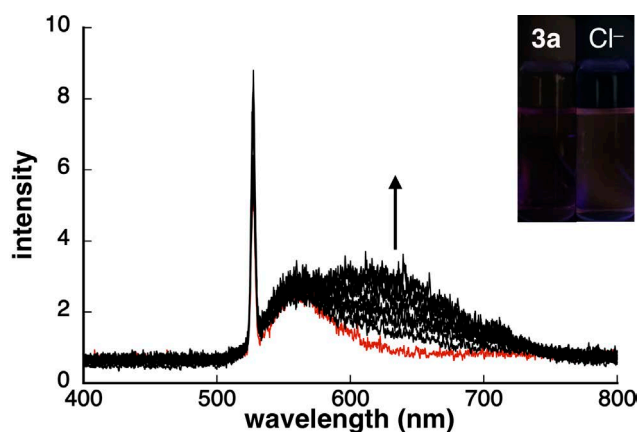


Fig. S29 (a) Fluorescence spectral changes of **3a** (1.0×10^{-5} M) upon the addition of Cl^- as a TBA salt (0–600 equiv) in CH_2Cl_2 (red lines: initial state of **3a**), excited at the absorption maximum of **3a**, and photographs under 365-nm UV light in the absence and presence of Cl^- (600 equiv) under the conditions for spectral measurements (inset). Φ_{FL} , obtained by the excitation at the absorption maximum, in **3a**· Cl^- was 0.002.

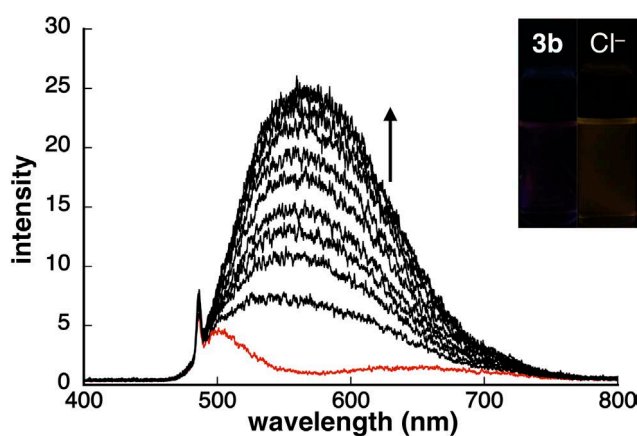


Fig. S30 (a) Fluorescence spectral changes of **3b** (1.0×10^{-5} M) upon the addition of Cl^- as a TBA salt (0–100 equiv) in CH_2Cl_2 (red lines: initial state of **3b**), excited at the absorption maximum of **3b**, and photographs under 365-nm UV light in the absence and presence of Cl^- (100 equiv) under the conditions for spectral measurements (inset). Φ_{FL} , obtained by the excitation at the absorption maximum, in **3b**· Cl^- was 0.069.

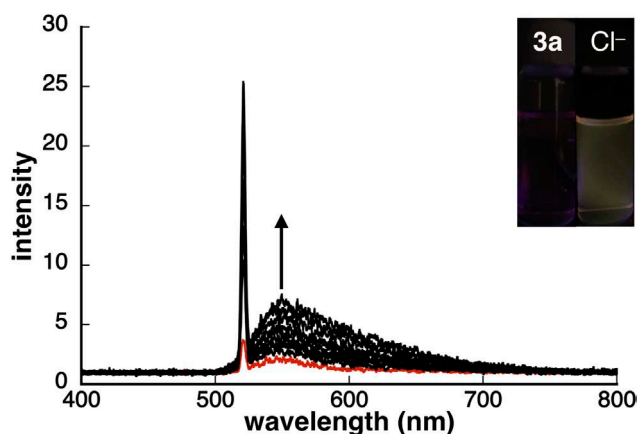


Fig. S31 (a) Fluorescence spectral changes of **3a** (1.0×10^{-5} M) upon the addition of Cl^- as a TBA salt (0–1500 equiv) in THF (red lines: initial state of **3a**), excited at the absorption maximum of **3a**, and photographs under 365-nm UV light in the absence and presence of Cl^- (1500 equiv) under the conditions for spectral measurements (inset). Φ_{FL} , obtained by the excitation at the absorption maximum, in **3a**· Cl^- was 0.031.

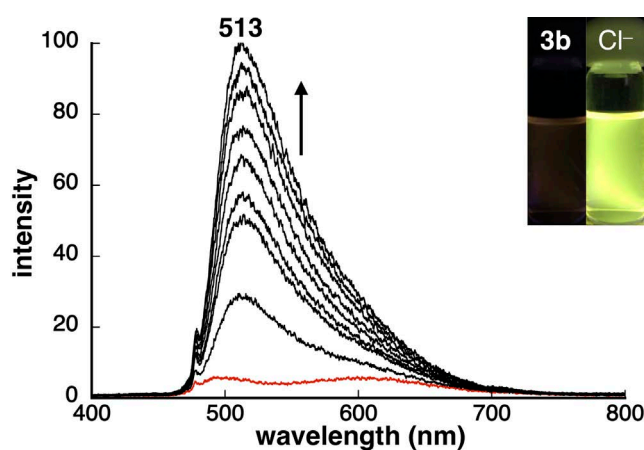


Fig. S32 (a) Fluorescence spectral changes of **3b** (1.0×10^{-5} M) upon the addition of Cl^- as a TBA salt (0–600 equiv) in THF (red lines: initial state of **3b**), excited at the absorption maximum of **3b**, and photographs under 365-nm UV light in the absence and presence of Cl^- (600 equiv) under the conditions for spectral measurements (inset). Φ_{FL} , obtained by the excitation at the absorption maximum, in **3b**· Cl^- was 0.15.

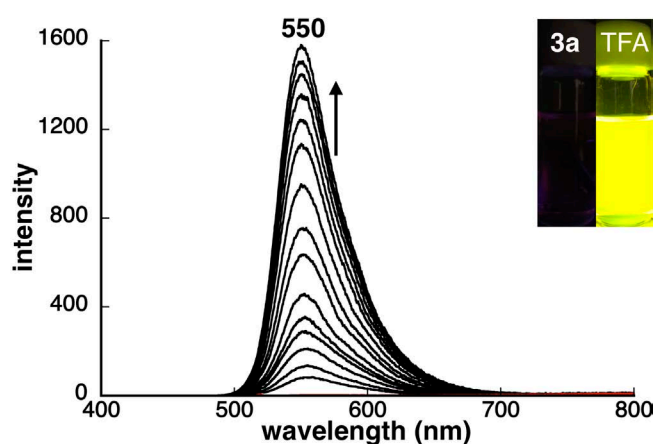


Fig. S33 (a) Fluorescence spectral changes of **3a** (1.0×10^{-5} M) upon the addition of TFA (0–100 equiv) in CH_2Cl_2 (red lines: initial state of **3a**), excited at the isosbestic point (510 nm) in the UV/vis absorption spectral changes, and photographs under 365-nm UV light in the absence and presence of TFA (100 equiv) under the conditions for spectral measurements (inset). Φ_{FL} , obtained by the excitation at the absorption maximum, in **3a**· 2H^+ was 0.82.

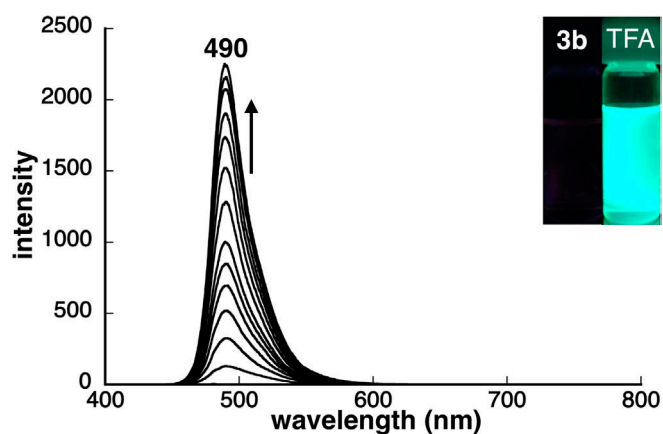


Fig. S34 (a) Fluorescence spectral changes of **3b** (1.0×10^{-5} M) upon the addition of TFA (0–100 equiv) in CH_2Cl_2 (red lines: initial state of **3b**), excited at the isosbestic point (480 nm) in the UV/vis absorption spectral changes, and photographs under 365-nm UV light in the absence and presence of TFA (100 equiv) under the conditions for spectral measurements (inset). Φ_{FL} , obtained by the excitation at the absorption maximum, in **3b**· 2H^+ was 0.76.

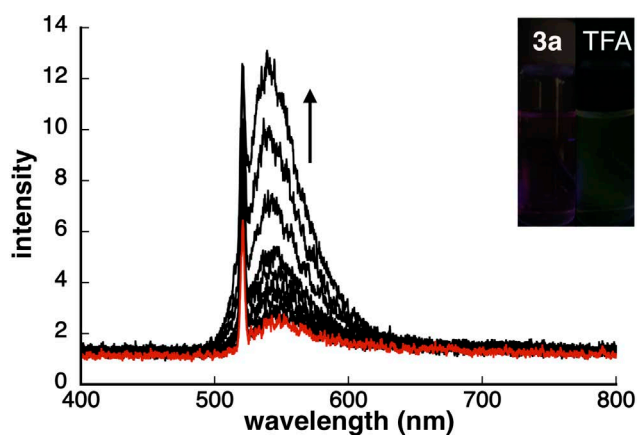


Fig. S35 (a) Fluorescence spectral changes of **3a** (1.0×10^{-5} M) upon the addition of TFA (0–9000 equiv) in THF (red lines: initial state of **3a**), excited at the absorption maximum of **3a**, and photographs under 365-nm UV light in the absence and presence of TFA (9000 equiv) under the conditions for spectral measurements (inset). Φ_{FL} , obtained by the excitation at the absorption maximum, in the presence of TFA could not be estimated due to the overlap between excited and emission bands.

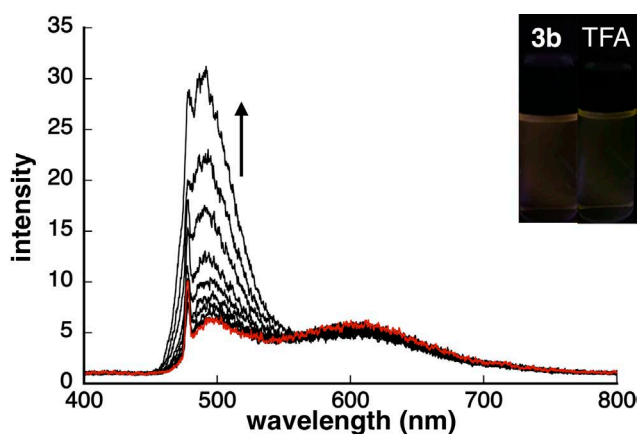


Fig. S36 (a) Fluorescence spectral changes of **3b** (1.0×10^{-5} M) upon the addition of TFA (0–9000 equiv) in THF (red lines: initial state of **3b**), excited at the absorption maximum of **3b**, and photographs under 365-nm UV light in the absence and presence of TFA (9000 equiv) under the conditions for spectral measurements (inset). Φ_{FL} , obtained by the excitation at the absorption maximum, in the presence of TFA was 0.027.

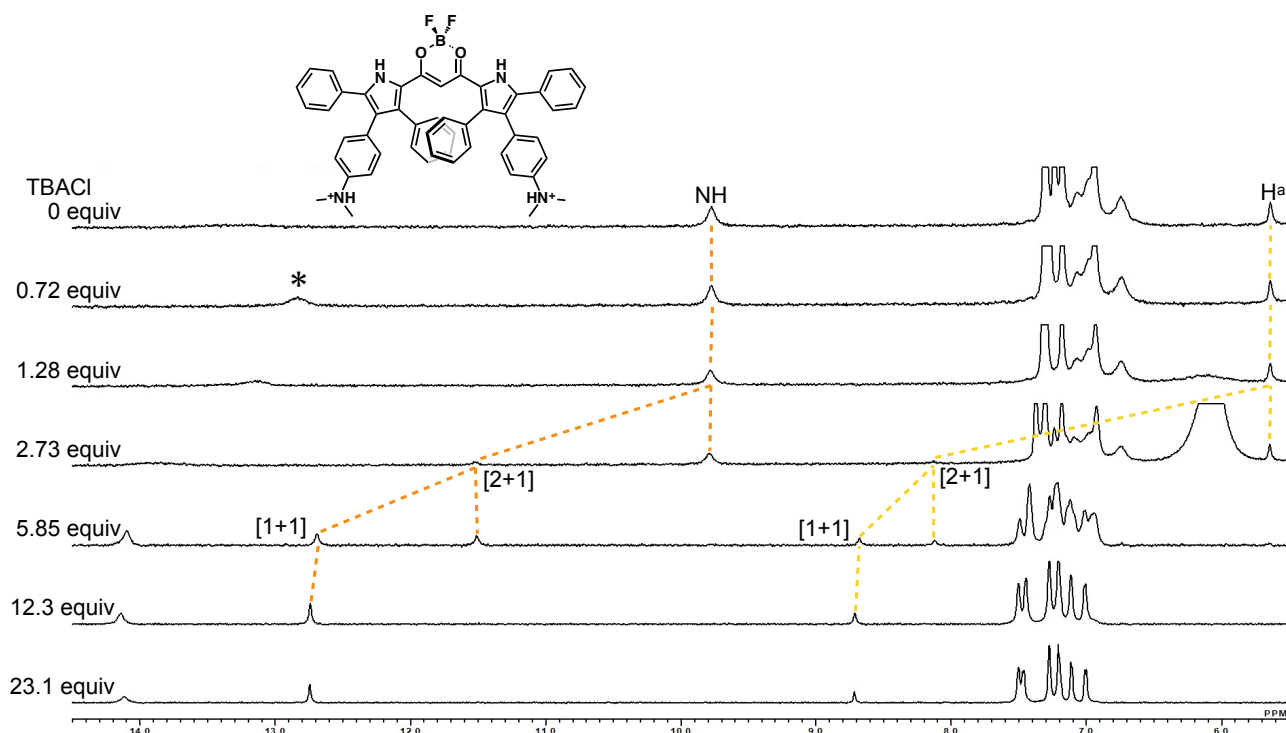


Fig. S37 ^1H NMR spectral changes of $3\mathbf{a}\cdot 2\text{H}^+$ (1×10^{-3} M) upon the addition of Cl^- as a TBA salt (0–23.1 equiv) in CD_2Cl_2 in the presence of TFA (5.0 equiv) at -50°C . The signals of pyrrole NH and bridging CH (H^{a}) gradually disappeared and new signals appeared concurrently in the downfield region, suggesting the formation of protonated $3\mathbf{a}\cdot\text{Cl}^-$ considered as $3\mathbf{a}\cdot\text{Cl}^- \cdot 2\text{H}^+$. On the other hand, the examinations for $3\mathbf{b}\cdot 2\text{H}^+$ could not be conducted because of the less solubility of protonated $3\mathbf{b}\cdot\text{Cl}^-$. The signal with asterisk was assigned to *N,N*-dimethylammonium NH by considering the integral and chemical shift. The signal ascribable to *N,N*-dimethylammonium NH (asterisk) were observed upfield due to the shielding effect of Cl^- binding (0–0.72 equiv), and the signal shifted downfield probably due to the interaction of *N,N*-dimethylammonium NH with excess Cl^- (0.72–23.1 equiv).

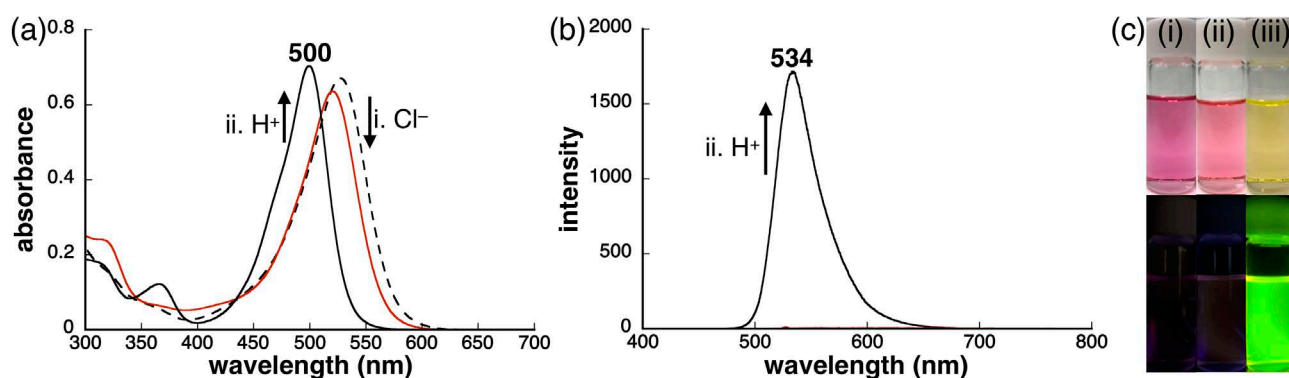


Fig. S38 (a)(i) UV/vis absorption and (b) fluorescence spectral changes of $3\mathbf{a}$ (1.0×10^{-5} M) upon the addition of TFA (100 equiv) in CH_2Cl_2 in the presence of Cl^- as a TBA salt (600 equiv), wherein broken and red lines showed $3\mathbf{a}$ and $3\mathbf{a}\cdot\text{Cl}^-$, respectively (UV/vis absorption spectral changes of $3\mathbf{a}$ upon the addition of Cl^- in CH_2Cl_2 : Fig. S21), and (c) photographs of (i) $3\mathbf{a}$, (ii) $3\mathbf{a}\cdot\text{Cl}^-$, and (iii) protonated $3\mathbf{a}\cdot\text{Cl}^-$ under visible light (top) and 365-nm UV light (bottom) under the conditions for spectral measurements. Φ_{FL} , obtained by the excitation at the absorption maximum, was 0.57 (protonated $3\mathbf{a}\cdot\text{Cl}^-$).

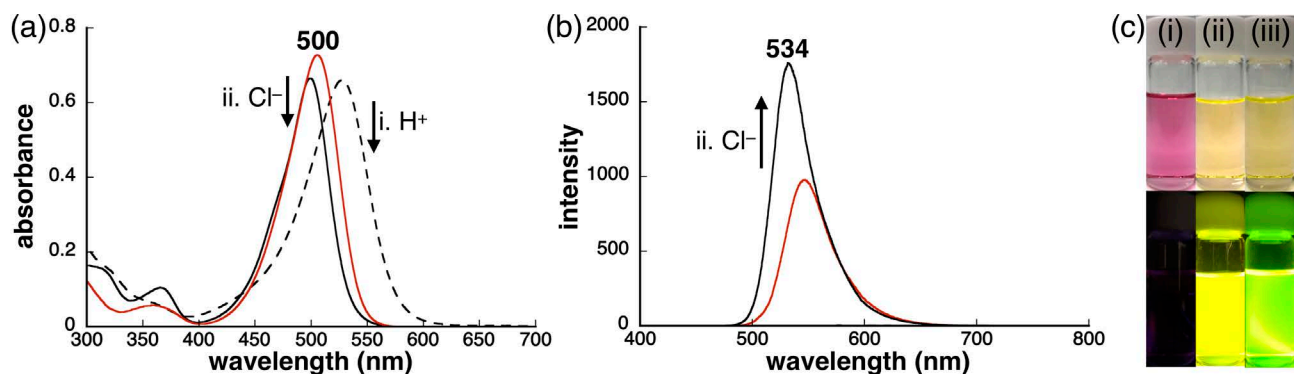


Fig. S39 (a) UV/vis absorption and (b) fluorescence spectral changes of **3a** (1.0×10^{-5} M) upon the addition of Cl^- as a TBA salt (600 equiv) in CH_2Cl_2 in the presence of TFA (100 equiv), wherein broken and red lines showed **3a** and **3a** $\cdot 2\text{H}^+$, respectively (UV/vis absorption spectral changes of **3a** upon the addition of TFA in CH_2Cl_2 : Fig. S25), and (c) photographs of (i) **3a**, (ii) **3a** $\cdot 2\text{H}^+$, and (iii) protonated **3a** $\cdot \text{Cl}^-$ under visible light (top) and 365-nm UV light (bottom) under the conditions for spectral measurements.

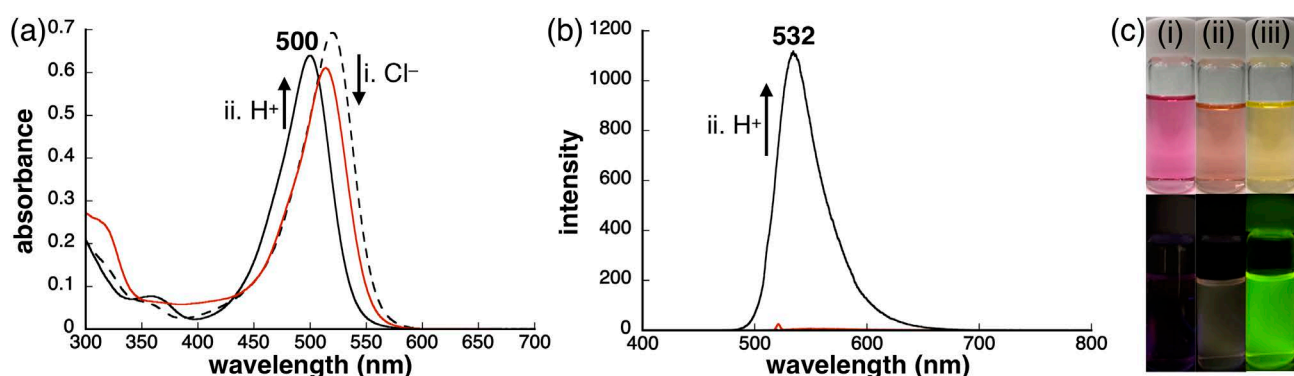


Fig. S40 (a)(i) UV/vis absorption and (b) fluorescence spectral changes of **3a** (1.0×10^{-5} M) upon the addition of TFA (9000 equiv) in THF in the presence of Cl^- as a TBA salt (1500 equiv), wherein broken and red lines **3a** and **3a** $\cdot \text{Cl}^-$, respectively (UV/vis absorption spectral changes of **3a** upon the addition of Cl^- in THF: Fig. S23), and (c) photographs of (i) **3a**, (ii) **3a** $\cdot \text{Cl}^-$, and (iii) protonated **3a** $\cdot \text{Cl}^-$ under visible light (top) and 365-nm UV light (bottom) under the conditions for spectral measurements. Φ_{FL} , obtained by the excitation at the absorption maximum, was 0.44 (protonated **3a** $\cdot \text{Cl}^-$).

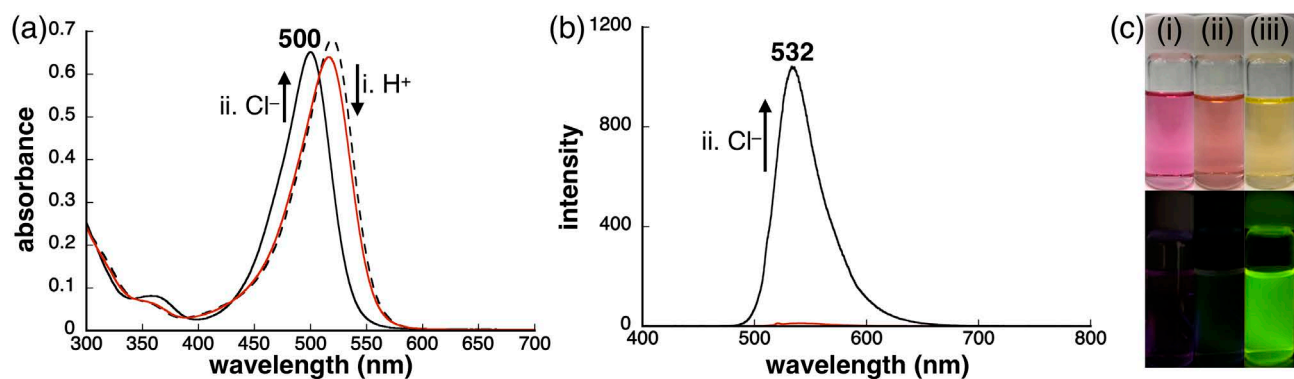


Fig. S41 (a) (i) UV/vis absorption and (b) fluorescence spectral changes of **3a** (1.0×10^{-5} M) upon the addition of Cl^- as a TBA salt (1500 equiv) in THF in the presence of TFA (9000 equiv), wherein broken and red lines showed **3a** in the absence and presence of TFA, respectively (UV/vis absorption spectral changes of **3a** upon the addition of TFA in THF: Fig. S27), and (c) photographs of (i) **3a**, (ii) **3a** in the presence of TFA, and (iii) protonated **3a** $\cdot \text{Cl}^-$ under visible light (top) and 365-nm UV light (bottom) under the conditions for spectral measurements.

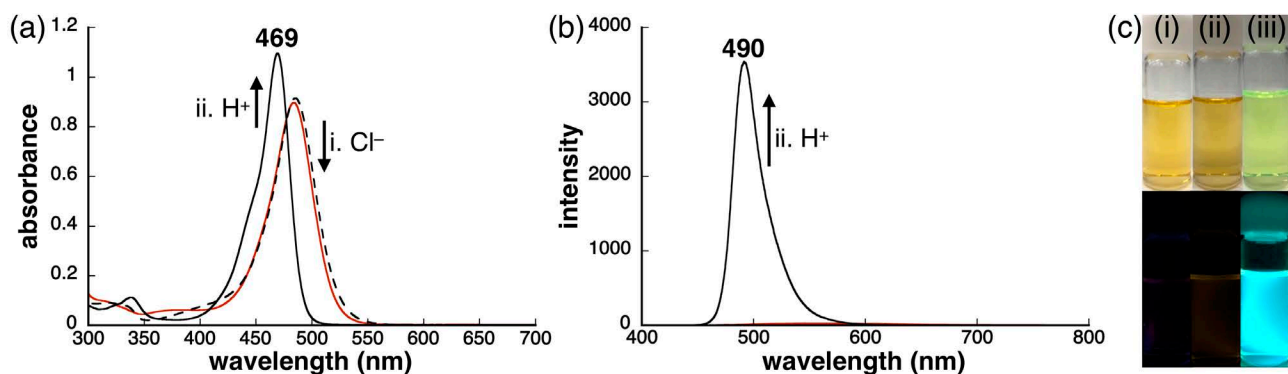


Fig. S42 (a)(i) UV/vis absorption and (b) fluorescence spectral changes of **3b** (1.0×10^{-5} M) upon the addition of TFA (100 equiv) in CH_2Cl_2 in the presence of Cl^- as a TBA salt (300 equiv), wherein broken and red lines showed **3b** and **3b**· Cl^- , respectively (UV/vis absorption spectral changes of **3b** upon the addition of Cl^- in CH_2Cl_2 : Fig. S22), and (c) photographs of (i) **3b**, (ii) **3b**· Cl^- , and (iii) protonated **3b**· Cl^- under visible light (top) and 365-nm UV light (bottom) under the conditions for spectral measurements. Φ_{FL} , obtained by the excitation at the absorption maximum, was 0.62 (protonated **3b**· Cl^-).

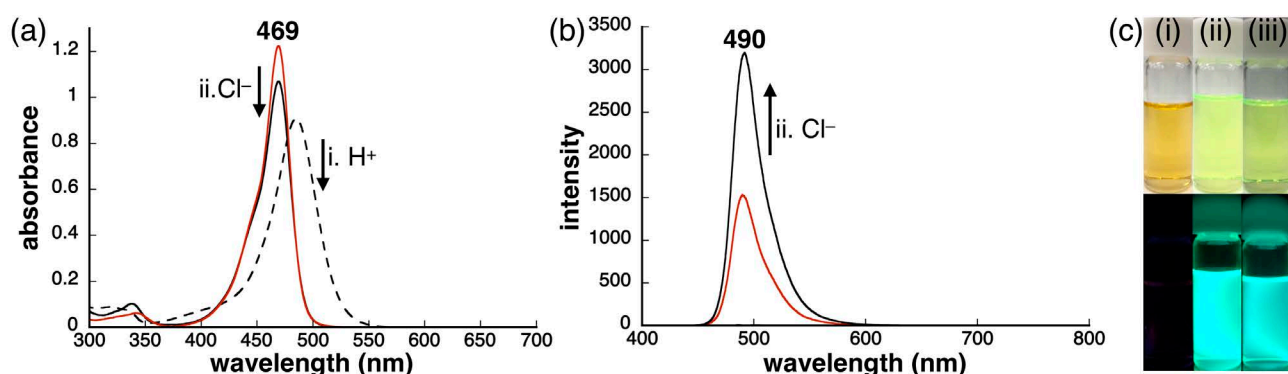


Fig. S43 (a)(i) UV/vis absorption and (b) fluorescence spectral changes of **3b** (1.0×10^{-5} M) upon the addition of Cl^- as a TBA salt (300 equiv) in CH_2Cl_2 in the presence of TFA (100 equiv), wherein broken and red lines showed **3b** and **3b**· 2H^+ , respectively (UV/vis absorption spectral changes of **3b** upon the addition of TFA in CH_2Cl_2 : Fig. S26), and (c) photographs of (i) **3b**, (ii) **3b**· 2H^+ , and (iii) protonated **3b**· Cl^- under visible light (top) and 365-nm UV light (bottom) under the conditions for spectral measurements.

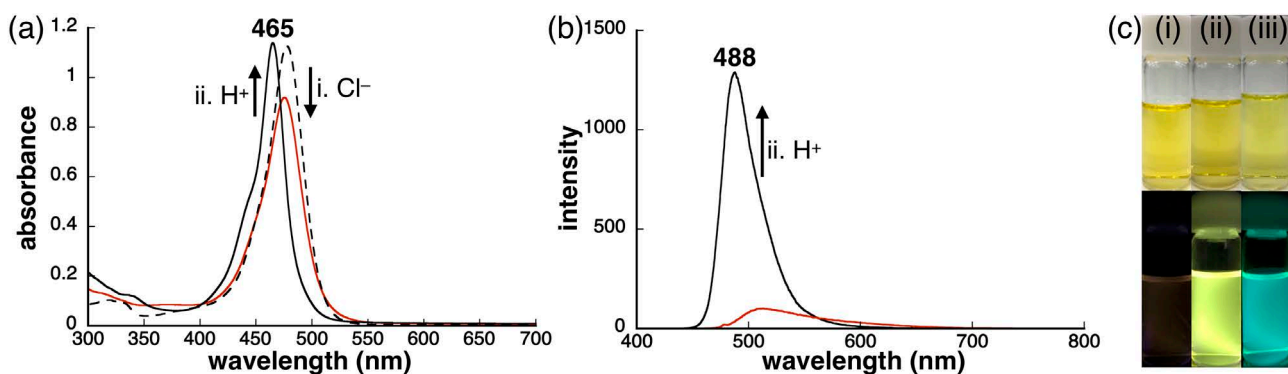


Fig. S44 (a)(i) UV/vis absorption and (b) fluorescence spectral changes of **3b** (1.0×10^{-5} M) upon the addition of TFA (9000 equiv) in THF in the presence of Cl^- as a TBA salt (600 equiv), wherein broken and lines showed **3b** and **3b**· Cl^- , respectively (UV/vis absorption spectral changes of **3b** upon the addition of Cl^- in THF: Fig. S24), and (c) photographs of (i) **3b**, (ii) **3b**· Cl^- , and (iii) protonated **3b**· Cl^- under visible light (top) and 365-nm UV light (bottom) under the conditions for spectral measurements. Φ_{FL} , obtained by the excitation at the absorption maximum, was 0.44 (protonated **3b**· Cl^-).

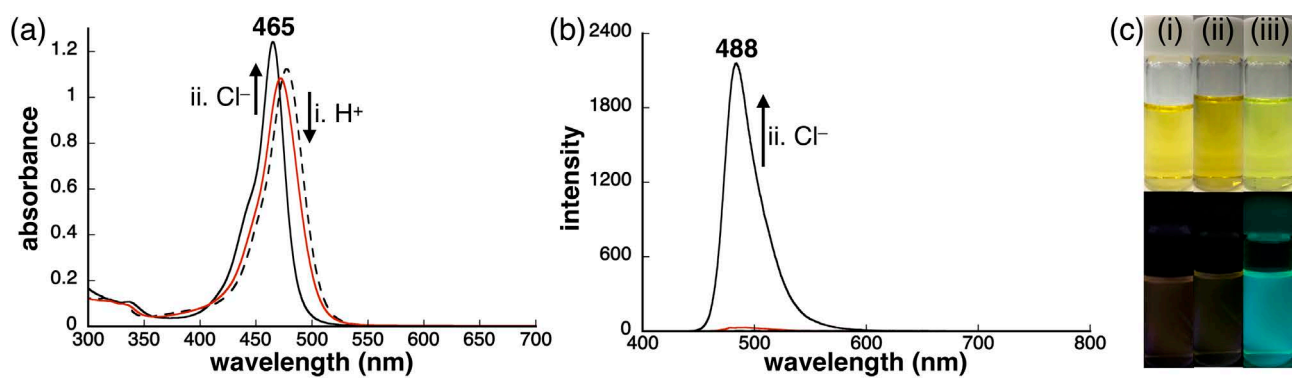


Fig. S45 (a)(i) UV/vis absorption and (b) fluorescence spectral changes of **3b** (1.0×10^{-5} M) upon the addition of Cl^- as a TBA salt (600 equiv) in THF in the presence of TFA (9000 equiv), wherein broken and red lines showed **3b** in the absence and presence of TFA, respectively (UV/vis absorption spectral changes of **3b** upon the addition of TFA in THF: Fig. S28), and (b) photographs of (i) **3b**, (ii) **3b** in the presence of TFA, and (iii) protonated **3b**· Cl^- under visible light (top) and 365-nm UV light (bottom) under the conditions for spectral measurements.

[S1] S. Sugiura, Y. Kobayashi, N. Yasuda and H. Maeda, *Chem. Commun.*, 2019, **55**, 8242–8245.